Stony Brook University

Synthesis of Polystyrene-*block*-poly(4-(phenylethynyl)styrene) (PS-*b*-PPES) Diblock Copolymers as Precursors for Cobalt-containing Materials

A Thesis Presented

by

Bin Qian

to

The Graduate School

in Partial Fulfillment of the

Requirements

for the Degree of

Master of Science

in

Chemistry

Stony Brook University

May 2014

Stony Brook University

The Graduate School

Bin Qian

We, the thesis committee for the above candidate for the

Master of Science degree, hereby recommend

acceptance of this thesis.

Robert B. Grubbs
Associate Professor, Chemistry Department

Kathlyn A. Parker
Professor, Chemistry Department

Peter Khalifah
Assistant Professor, Chemistry Department

This thesis is accepted by the Graduate School

Charles Taber
Dean of the Graduate School

Abstract of the Thesis

Synthesis of Polystyrene-*block*-poly(4-(phenylethynyl)styrene) (PS-*b*-PPES) Diblock Copolymers as Precursors for Cobalt-containing Materials

by

Bin Qian

Master of Science

in

Chemistry

Stony Brook University

2014

Block copolymers consist of two or more homopolymer units linked by a covalent bond. They have attracted great research interest because they can microphase separate to form highly ordered nanostructures. The well-defined nanoscale metal-polymer hybrid materials can be formed through self-assembly and phase separation of alkyne-functional polymers with metal species that can react with the alkyne groups, which may have potential applications for memory storage, energy storage, and biomedical equipment. The focus of this thesis is the synthesis of polystyrene-*block*-poly(4-(phenylethynyl)styrene) (PS-*b*-PPES) diblock copolymers as precursors for cobalt-containing materials.

Polystyrene-*block*-poly(4-(phenylethynyl)styrene) (PS-*b*-PPES) diblock copolymers were synthesized at a variety of PS/PPES ratios by reversible addition-fragmentation chain transfer (RAFT) polymerization. Macro chain transfer agent (mCTA) was achieved by RAFT polymerization of polystyrene (PS) with chain transfer agent (CTA), *S*-α-

(Methoxycarbonyl)phenylmethyl dithiobenzoate (MCPDB). PS-*b*-PPES diblock copolymers were subsequently prepared by RAFT polymerization of 4-(phenylethynyl)styrene (4-PES) with the PS-mCTA. Copolymer samples were treated with one equivalent of cobalt carbonyl ($Co_2(CO)_8$) compound per alkyne unit at room temperature to form cobalt-polymer hybrid materials.

Proton nuclear magnetic resonance (^{1}H NMR) spectroscopy and gel permeation chromatography (GPC) were applied to analyze the PS-mCTA and diblock copolymer products. The miscibility of poly(4-(phenylethynyl)styrene) (PPES) with PS in diblock copolymers with different compositions was characterized by differential scanning calorimetry (DSC). The loss of CO from cobalt-copolymer adducts was monitored by IR spectroscopy after heating in bulk at 110 ℃ for 24 hours. Transmission electron microscopy (TEM) was used to investigate the phase separation of the self-assembled cobalt-polymer hybrid materials, which appears to form cylindrical morphologies for different compositions (PS_{89}-$PPES_{23}[Co_2(CO)_6]_{21}$, PS_{89}-$PPES_{41}[Co_2(CO)_6]_{37}$, PS_{125}-$PPES_{51}[Co_2(CO)_6]_{46}$, and PS_{125}-$PPES_{125}[Co_2(CO)_6]_{112}$). Increasing the length of PS and PPES blocks leads to an increase in the size of the each domain. In addition, PS_{89}-$PPES_{23}[Co_2(CO)_6]_{21}$ and PS_{125}-$PPES_{125}[Co_2(CO)_6]_{112}$ both form cylinders, but for PS_{89}-$PPES_{23}[Co_2(CO)_6]_{21}$, polystyrene is the majority domain; and for PS_{125}-$PPES_{125}[Co_2(CO)_6]_{112}$, polystyrene is the minority domain.

Table of Contents

List of Figures

List of Tables

List of Abbreviations

^{1}H NMR — proton nuclear magnetic resonance
4-PES — 4-(phenylethynyl)styrene
AIBN — *2,2*-Azobisisobutyronitrile
ATRP — atom-transfer radical polymerization
BCPs — block copolymers
CRP — controlled free radical polymerization
CTA — chain transfer agent
DMF — *N*,*N*-dimethylformamide
DSC— differential scanning calorimetry
GPC — gel permeation chromatography
IR— infrared spectroscopy
mCTA — macro chain transfer agent
MC-BCPs — metal-containing block copolymers
MCPDB — *S*-α-(Methoxycarbonyl)phenylmethyl dithiobenzoate
MCPs — metal-containing polymers
M_n — number average molecular weight
M_w — weight average molecular weight
NMP — nitroxide-mediated Radical polymerization
PS — polystyrene
PS-*b*-PPES — polystyrene-*block*-poly(4-(phenylethynyl)styrene)
PS-*b*-PMMA — polystyrene-*block*-poly(methylmethacrylate)
RAFT — reversible addition-fragmentation chain transfer
SAXS — small-angle X-ray scattering
TEM — transmission electron microscopy
T_g — glass transition temperature
THF — tetrahydrofuran

Acknowledgments

I would like to thank Professor Grubbs, my research supervisor, for all the advice and support for my lab work in the past two years. I would also like to thank Bingyin for training me for my research, and thank him and Kim Kisslinger for helping me acquire the TEM images. My grateful thanks are also extended to my group members Tianyuan, Zhe, Rui, Menglan, Daniel, Deokkyu, Scott, and David for their cooperation in the lab. Special thanks should be given to Jim Marecek for his training and help with the NMR instrumentation. I also need to thank Professor Chu and Hsiao to approve me to use DSC instrument in their lab.

I would also like to extend my thanks to Katherine Hughes, Professor Drueckhammer, and the chemistry department faculties for their help and guidance through my academic career.

Introduction

1. Metal-containing Block Copolymers (MC-BCPs)

The metal-containing polymers (MCPs) have attracted intense research interest as they have great potential applications in optoelectronic materials, magnetic materials, or as precursors to ceramics and metallic nanoparticles.[1-3] The approaches to prepare such polymer-metal hybrid materials have also been advanced by many research. The conventional methods, also called "top-down" techniques,[4] include photolithography, electron-beam lithography, and X-ray lithography which are usually limited by complicated steps and high cost. Conversely, the "bottom-up" techniques, such as incorporation of metal elements into self-assembled block copolymers (BCPs), are cost-effective and rapid methods.[4] In addition, the MC-BCPs have great advantages in controlling the structure of materials on the nanoscale through the localization of metal aggregates to well-defined nanometer-scale domains as lithographic methods are limited by the properties of the photoresist and the wavelengths of radiation used in patterning process.[5]

Different strategies are applied to prepare such MCPs.[5-8] The first approach is direct polymerization of metal-functional monomers to MCPs, but its applications are restricted by the limited stability of metal-containing monomers. The second approach is direct assembly of block copolymers with nanoscale metal aggregates. This is the most convenient method, however, it depends on limited nanoparticles to specific copolymers.[5] The third approach is ligation of metals to ligand-functional block copolymers, where block copolymer micro-phase separation enables ligand functional groups to occupy well-defined spatial regions in the bulk, which

provides the potential for ordered and stabilized metal nanoparticles. In our approach, nanoparticle precursors are incorporated into the alkyne-functional block copolymers and then the nanoparticles are prepared in the bulk material.

2. Diblock Copolymers

Block copolymers (BCPs) contain two or more immiscible homopolymer units linked by a covalent bond. Diblock copolymers are the simplest form of BCPs and the complexity of the system increases with the increasing number of blocks.[8-9] The incompatibility between the two blocks results in the micro phase separation of diblock copolymers, forming various structures with domains in nanometer scale. A lot of research has been done to study the self-assembly of block copolymers.[10-13] Figure 1[14] shows different morphologies of the diblock copolymer, polystyrene-*block*-poly(methylmethacrylate) (PS-*b*-PMMA), represented as simplified two-color chains. The structures are determined primarily by the relative lengths of the polymer block A (f_A) and the periodic equilibrium phases for diblock copolymers, with increasing fraction of block A, include spheres, cylinders, gyroid, and lamellae.

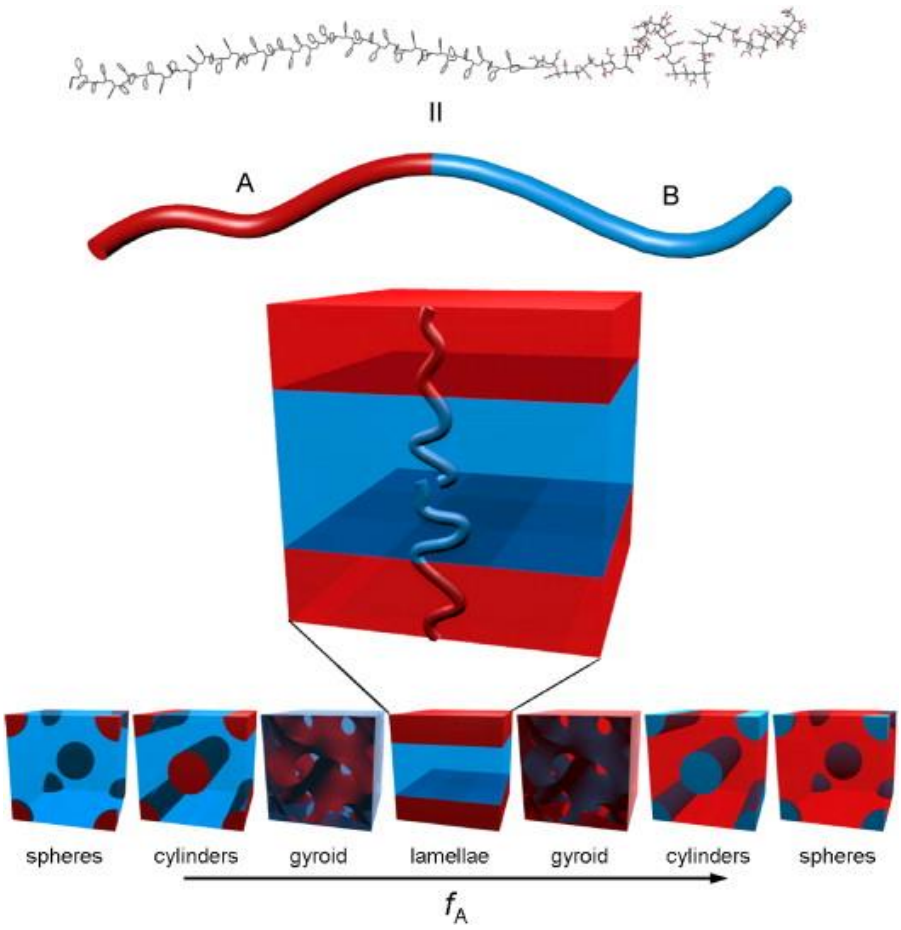

Figure 1. The A–B diblock copolymer, PS-*b*-PMMA, with spherical, cylindrical, gyroidal, and lamellar structures. Reprinted from Progress in Polymer Science, 32 / 10, S.B. Darling, Directing the self-assembly of block copolymers / Introduction to block copolymers, Pages No.1154, Copyright (2007), with permission from Elsevier.

In addition, further studies have demonstrated that the phase diagram (Figure 2) of diblock copolymers is mainly controlled by the degree of polymerization (N), Flory-Huggins interaction parameter (χ), and the volume fraction of the block A (f_A).[15] In Figure 2, with increasing volume fraction (f) of one block, the structures include spherical (CPS/Q^{229}), cylindrical (H), gyroidal (Q^{230}) and lamellar structures (L). The quantity of the product χN, also known as degree of incompatibility, indicates whether the phase-separation will happen. The higher the χ, the more likely phase separation will happen.

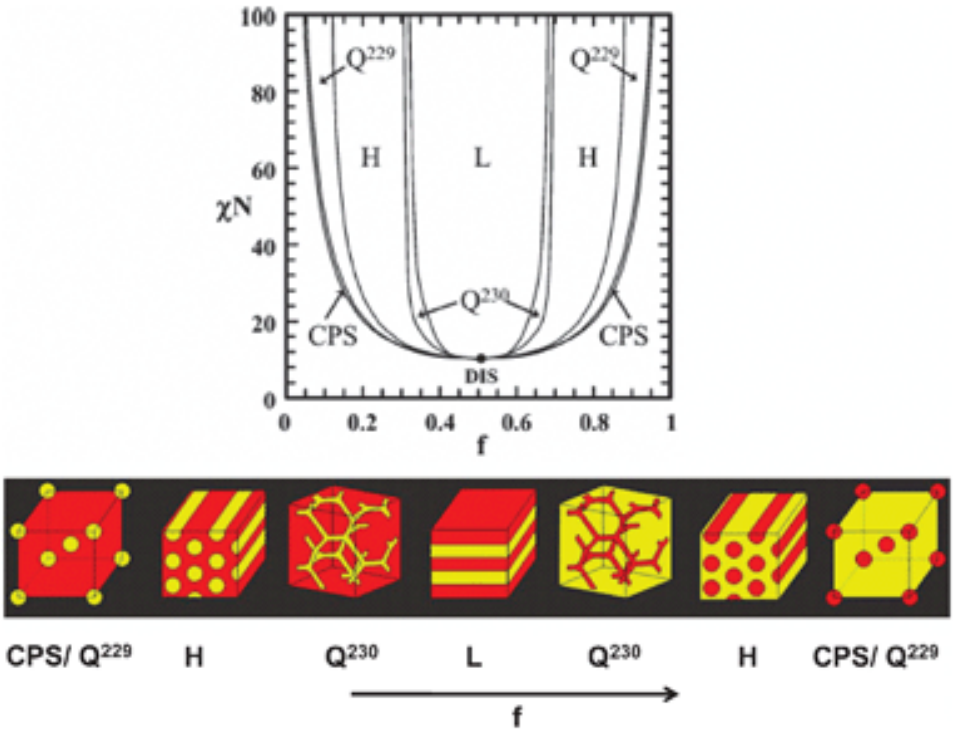

Figure 2. Theoretical phase-diagram of a diblock copolymer (top) and illustrations of the resulting morphologies (bottom). Reproduced in part from {M. Christopher Orilall and Ulrich Wiesner, *Chem. Soc. Rev.* **2011**, *40*, 520−535.} with permission of The Royal Society of Chemistry.

Increasing the number of blocks (triblock and tetrablock copolymers) and or changing the polymer architecture (linear, star and brush copolymers) increase the complexity of the phase diagram and can result in the formation of additional micro-structures.[16-17]

In this thesis, the polystyrene-*block*-poly(4-(phenylethynyl)styrene)(PS-*b*-PPES) system is prepared by reversible addition-fragmentation chain transfer (RAFT) polymerization as precursor for MC-BCPs. The miscibility of PPES with PS was proved by previous DSC studies.[18] The blend of homopolymers PS and PPES, and PS-*b*-PPES diblock copolymer were characterized to prove a high degree of miscibility by DSC profiles. In this thesis, the miscibility of a wide range of PS-*b*-PPES diblock copolymers (3.4 kg/mol ≤ M_n ≤ 38.6 kg/mol; 16 wt % ~ 84 wt % PPES) were confirmed by DSC studies.

3. Reversible Addition-fragmentation Chain Transfer (RAFT) Polymerization

Recent advances have been witnessed for synthesis of well-defined polymers. Controlled free radical polymerization (CRP) techniques have opened new approaches for materials science.[19] These new techniques facilitate the development of new materials by improving the versatility and compatibility of controlled polymerization techniques with range of monomers and functional groups. So far, the most significant CRP techniques could be classified as nitroxide-mediated radical polymerization (NMP),[20] atom-transfer radical polymerization (ATRP),[21-22] and RAFT polymerization.[23-25] The oldest one is NMP approach that makes use of alkoxyamine initiators for the synthesis of homopolymers and block copolymers with very low polydispersity index, though still limited by difficult synthesis of alkoxyamines and incompatibility with many important monomer families.[26] ATRP which has been proven to be more versatile is a transition metal-mediated polymerization that can be run in a range of non-aqueous solvents, aqueous systems, or in neat monomer.[21] RAFT polymerization is one of the most convenient and versatile approaches for the design and synthesis of novel materials. It has many advantages, including compatibility with the majority of monomers used with radical polymerization, retention of end groups that allows future modification of chain ends, and narrow molecular weight distributions for the synthesized polymers.[23]

Initiation

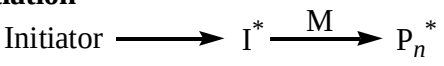

Reversible chain transfer

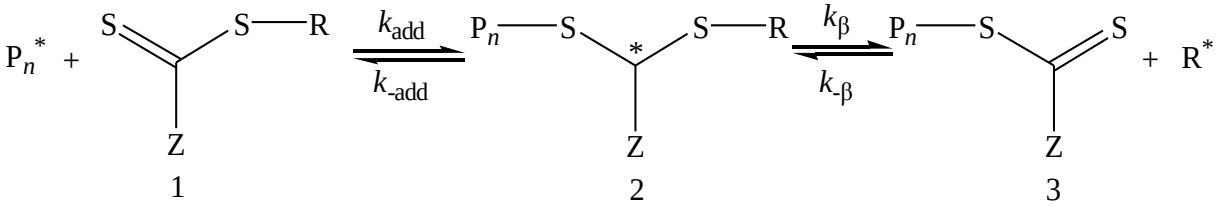

Reinitiation

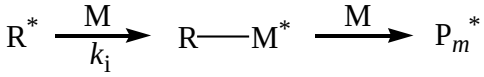

Chain equilibration

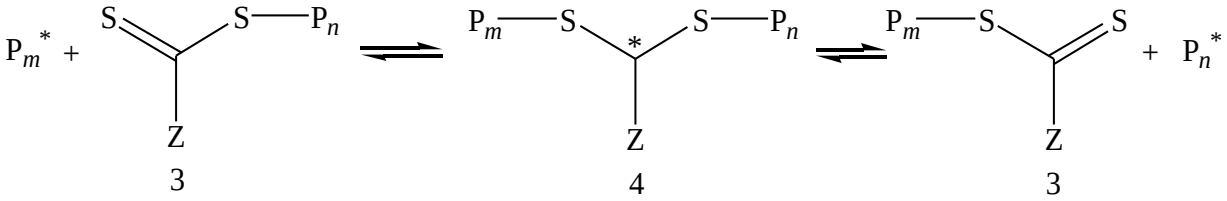

Termination

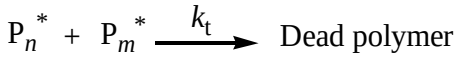

Figure 3. Mechanism of RAFT polymerization.

The mechanism of RAFT polymerization is shown in Figure 3.[23] The initiation step is like that in a conventional radical polymerization with very low concentration of free radical (I^*) and thus very low concentration of propagating radical (P_n^*). In the reversible chain transfer step, the propagating radical (P_n^*) reacts with a thiocarbonylthio compound **1**, also known as a chain transfer agent (CTA), to form an intermediate radical **2**, which can then fragment into a polymeric thiocarbonylthio compound **3**, also known as macro-chain transfer agent (mCTA), and a new radical (R^*). Reinitiation occurs by reaction of the radical (R^*) with monomers (M) to form a new propagating radical (P_m^*). Then, an equilibration is reached between propagating radicals (P_n^* and P_m^*) and the dormant mCTA **3**; the intermediate radical **4** can fragment in either

direction which gives the same chance for all polymer chains to grow, resulting in uniform chain growth and thus narrow molecular weight distribution.[27] At last, when polymerization is stopped, the thiocarbonylthio end groups could be preserved on the isolated products that allows future modification on chain ends.[28] Because the free radicals are not consumed during the reversible chain transfer step, reinitiation step, and chain equilibration step, in spite of radical-radical termination and other side reactions, the concentration of free radicals in the system only depends on the first initiation step, while the rate of polymerization is independent of the concentration of RAFT agent. The rate constant for chain transfer (k_{tr}) is defined as equation (1)[29]:

$$\boldsymbol{k_{tr} = k_{add}\frac{k_{\beta}}{k_{-add}+k_{\beta}}} \qquad (1)$$

And the theoretical molecular weight of the polymer product is given by equation (2)[28]:

$$\boldsymbol{M_{n,\ theoretical} = \frac{[M]_0 \times MW_{monomer} \times p}{[CTA]_0} + MW_{CTA}} \qquad (2)$$

Where $[M]_0$ is the initial monomer concentration, $MW_{monomer}$ is the monomer's molecular weight, p is the conversion, MW_{CTA} is molecular weight of the chain transfer agent, and $[CTA]_0$ is the initial concentration of CTA.

One key point for successful RAFT process is the choice of RAFT agent or chain transfer agent (CTA). Many families of thiocarbonylthio compounds have been reported as RAFT CTAs in the literature.[30-32]

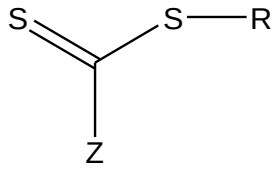

Figure 4. RAFT agent or CTA.

The efficiency of these RAFT agent is mainly dependent on the so-called Z and R groups (Figure 4). Group Z could influence the activity of the C=S bond and stabilize the intermediate radicals, while more reactive C=S bond means higher k_{add} and intermediate radicals could fragment rapidly without any side reaction if S–R bond is weak. As a result, group R should be a good leaving group, additionally, must be able to reinitiate polymerization.[23, 27,29] The selection for monomers is also very important that the monomers should not only contain functional groups for future modification but also could stabilize the propagating radicals that drives the reaction.[28-29] Figure 5 and 6 show the RAFT chain transfer agent (CTA), *S*-α-(Methoxycarbonyl)phenylmethyl dithiobenzoate (MCPDB), and the monomer, 4-(phenylethynyl)styrene (4-PES), used in this work. The reason of selective CTA is that the phenyl group could stabilize the intermediate radical because of its conjugated structure, in addition, the methyl phenylacetate group is not only a good leaving group but also can reinitiate monomers.

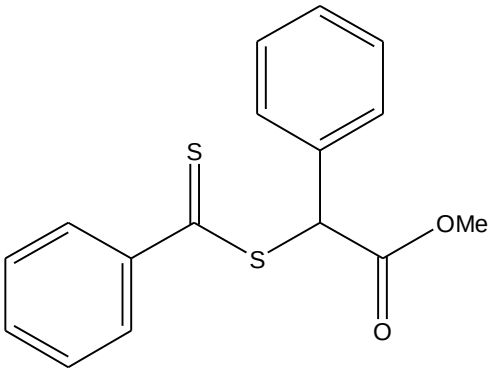

Figure 5. *S*-α-(Methoxycarbonyl)phenylmethyl dithiobenzoate (MCPDB), RAFT chain transfer agent (CTA).

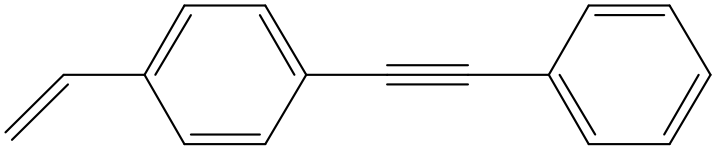

Figure 6. 4-(Phenylethynyl)styrene (4-PES), the monomer used for RAFT.

RAFT polymerization can be carried over a wide range of temperature and in various solvents, including aqueous solution.[33] The selection of solvent depends on what kind of monomer is used. For this work, RAFT polymerization is carried out in anisole solution, due to its high boiling point (154 ℃) and its ability to dissolve all the reaction components, including monomer, CTA, initiator and products. The reaction temperature should be well controlled because increasing the temperature will not only increase the polymerization rate but also increase the possibility of radical-radical termination or other side reactions. In addition, the reaction time must be adjusted according to the conversion of monomers monitored by ^{1}H NMR spectrum.

4. Motivation

In this thesis, polystyrene-*block*-poly(4-(phenylethynyl)styrene) (PS-*b*-PPES) diblock copolymers were prepared as precursors for cobalt-containing materials by RAFT polymerization. The phase separation of diblock copolymers allowed the metallic domains to form ordered morphologies after selective incorporation of dicobalt octacarbonyl ($Co_2(CO)_8$) in the alkyne functional PPES blocks. A series of diblock copolymers with different PS/PPES ratios were prepared and phase-separation behavior of their cobalt adducts was characterized by transmission electron microscopy (TEM). Different morphologies were mapped in association with different compositions. Thermolysis of carbonyl groups from the cobalt-containing diblock copolymers after heating was observed by IR spectroscopy and the miscibility of PPES block with PS block in copolymers could be observed by differential scanning calorimetry (DSC).

Experimental Section

Materials

4-Bromobenzyl bromide (98+%, Alfa Aesar), triphenylphosphine (99%, Alfa Aesar), sodium hydroxide (pellets, 97.0%, EMD), formaldehyde (36.5-38.0% aqueous solution, Macron), phenylacetylene (98%, Acros), copper (I) iodide (98%, Alfa Aesar), triethylamine (99+%, J.T. Baker), bis(triphenylphosphine)palladium(II)chloride (98%, Acros), phenylmagnesium bromide (3M in diethyl ether, Alfa Aesar), carbon disulfide (99.97%, EMD), methyl α-bromophenylacetate (97.0+%, TCI), chloroform (99%, J.T. Baker), hexanes (98.5%, BDH), *N*,*N*-dimethylformamide (99.8%, EMD) (DMF), dichloromethane (99.8%, BDH), tetrahydrofuran (99.9%, EMD) (THF), methanol (99.8%, VWR), diethyl ether (99.5%, Macron), sodium chloride (99%, J.T. Baker), magnesium sulfate (anhydrous, J.T. Baker), sodium sulfate (anhydrous, J.T. Baker), silica gel (0.035-0.070 mm, Acros), and dicobalt octacarbonyl (stabilized with 1-5% hexane, Alfa Aesar) were used as received. Hydrochloric acid (36.5-38.0% aqueous solution, J.T. Baker) was diluted from ~12M down to 2M before use. Toluene (anhydrous, 99.8%, Acros) was stored under N_2. *2,2*-Azobisisobutyronitrile (98%, Aldrich) (AIBN) was recrystallized from methanol and stored in a freezer. Styrene (stabilized, 99.9%, Fisher) was distilled at reduced pressure to remove radical inhibitors before use. Anisole (99%, Alfa Aesar) was passed through basic alumina columns and stored over molecular sieves (pore size 3 Å).

Instrumentation

^{1}H NMR Spectroscopy. ^{1}H NMR (300 MHz) spectra were recorded on a Bruker Fourier 300 NMR Spectrometer at 25 ℃ and *d*-chloroform was used as the solvent.

Gel permeation chromatography. GPC runs were conducted at 40 ℃ with THF (HPLC grade, J.T. Baker) as the eluent at a flow rate of 1.0 mL/minute. The GPC consisted of a K-501 pump (Knauer), a K-3800 Basic Autosampler (Marathon), 2 × PLgel 5 μm Mixed-D columns (300 × 7.5 mm, rated for linear separations at polymer molecular weights from 200 to 400,000 g/mol Polymer Laboratories), a CH-30 Column Heater (Eppendorf), a PL-ELS 1000 Evaporative Light Scattering Detector (Polymer Laboratories) and a PL Datastream unit (Polymer Laboratories). Narrow polydispersity polystyrene standards with molecular weights from 580-377,400 g/mol (EasiCal PS-2, Polymer Laboratories) were applied to analyze data.

Differential scanning calorimetry. DSC measurements were carried out under N_2 purge gas (20 mL/min) using a Perkin Elmer DSC7 instrument. All experiments were heated from 0 ℃ to 200 ℃ at 10 ℃/min and cooled from 200 ℃ to 0 ℃ at the same rate for two cycles. The onset of the T_g was measured from second heating scan.

Infrared spectroscopy. IR spectroscopy was carried out on a Nicolet iS10 (Thermo scientific) equipped with a Smart iTR Diamond Attenuated Total Reflectance cell.

Transmission electron microscopy. TEM imaging was performed using a JEOL-1400 transmission electron microscope at 80 kV at Center for Functional Nanomaterials (CFN) in Brookhaven National Laboratory (BNL).

Preparation of monomer: 4-(phenylethynyl)styrene (4-PES)

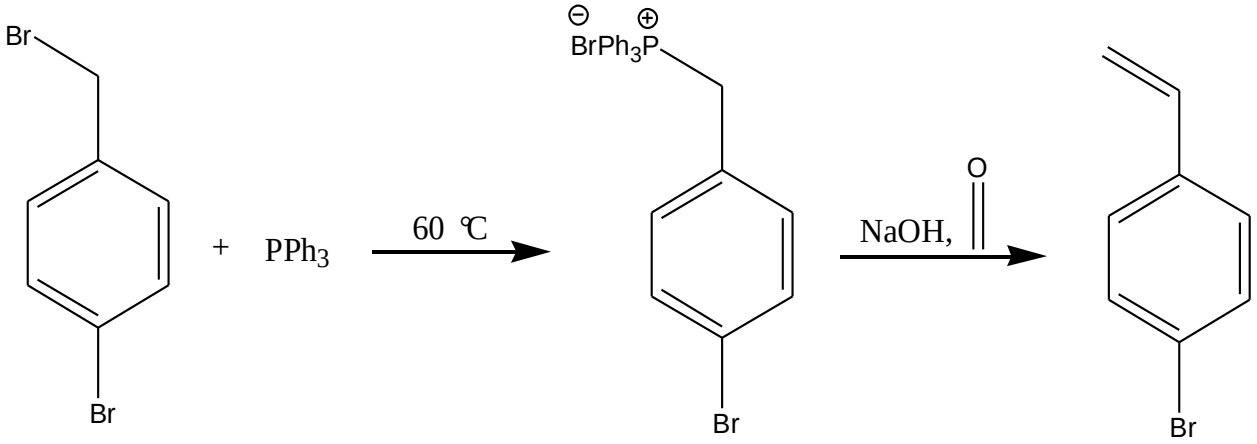

Figure 7. Synthesis of 4-bromostyrene by Wittig reaction.[34]

4-Bromobenzyl bromide (10.01 g, 0.04 mol) and triphenylphosphine (10.40 g, 0.04 mol) were dissolved in 100 mL of chloroform and stirred at 60 ℃ for 5 hours. After reaction, the solvent was removed by rotatory evaporator. The solid was rinsed with 100 mL diethyl ether, and the residue was dried under vacuum oven overnight at 20 ℃ to afford a white solid. The resulting intermediate product was treated with sodium hydroxide (4.25 g, 0.11 mol) in 100 mL formaldehyde solution at room temperature for 72 hours. After reaction, the solution was extracted with 3 × 200 mL hexanes, with a white sludge appearing in the water layer. The combined hexanes layers were dried with magnesium sulfate overnight. Magnesium sulfate was filtered and hexanes was evaporated to afford a colorless and transparent solution. After column chromatography on silica gel (particle size, 0.035-0.070 mm) with hexanes as the eluent, the desired product was obtained (6.49 g, overall yield 88.7%). ^{1}H NMR (300 MHz, $CDCl_3$): δ 7.27-7.49 (m, 4H, Ar-H), 6.67 (dd, 1H, J = 10.9 Hz and 17.6 Hz, =CH-Ar), 5.76 (d, 1H, J = 17.6 Hz, *trans* CH_2=CH-), 5.30 (d, 1H, J = 10.9 Hz, *cis* CH_2=CH-).

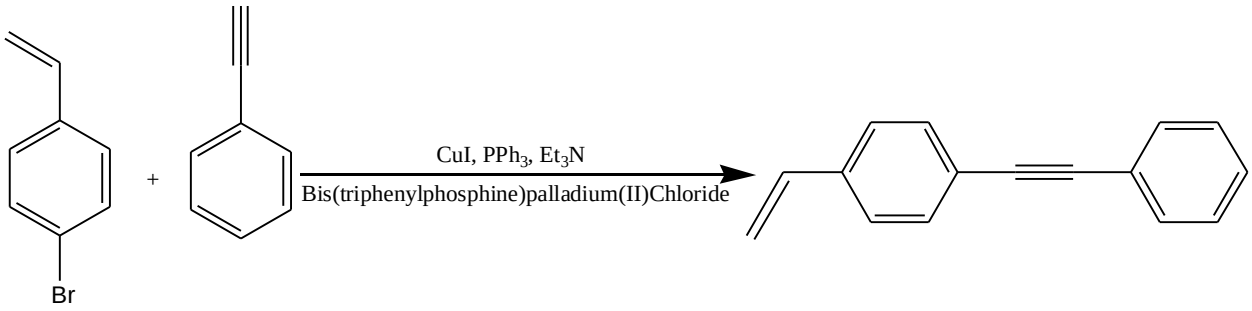

Figure 8. Synthesis of 4-(phenylethynyl)styrene via Sonogashira coupling.[35]

4-Bromostyrene (14.86 g, 81 mmol), phenylacetylene (12.26 g, 120 mmol), copper (I) iodide (0.20 g, 0.8 mmol), and triphenylphosphine (0.22 g, 0.8 mmol) were dissolved in dry triethylamine (150 mL) and bubbled with nitrogen for 1 hour at room temperature. Bis(triphenylphosphine)palladium(II)chloride (0.58 g, 0.8 mmol) was added to the solution, and the mixture was stirred at 70 ℃ for 76 hours under nitrogen protection. After reaction, the brown triethylammonium salt precipitate was filtered and triethylamine was evaporated. The orange-red residue was then dissolved in 150 mL hexanes, and the solution was washed with 40mL H_2O + 40 mL HCl (2 mol/L) + 40 mL brine. The mixture was extracted with hexanes and dried with $MgSO_4$ overnight. After filtration of $MgSO_4$ and evaporation of hexanes, thin layer chromatography (TLC) was tested with hexanes as the solvent, showing product spot is colorless with R_f = 0.474. The mixture was separated by column chromatography on silica gel (particle size, 0.035-0.070 mm) with hexanes as the eluent. The desired product was purified by recrystallization in methanol to afford faintly yellow crystals (11.78 g, yield 71.0%). ^{1}H NMR (300 MHz, $CDCl_3$): δ 7.27 – 7.57 (m, 9H, Ar-H), 6.74 (dd, 1H, J = 10.9 and 17.6 Hz, =CH-Ar), 5.81 (d, 1H, J = 17.6 Hz, *trans* CH_2=CH-), 5.32 (d, 1H, J = 10.9 Hz, *cis* CH_2=CH-).

Preparation of RAFT chain transfer agent (CTA): *S*-α-(Methoxycarbonyl)phenylmethyl dithiobenzoate (MCPDB)[36]

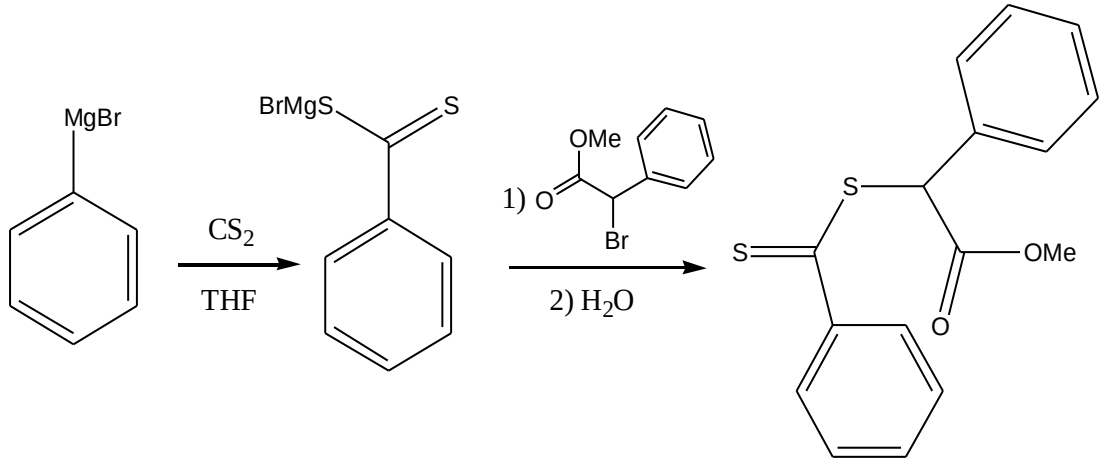

CTA, MCPDB

Figure 9. Synthesis of CTA, *S*-α-(Methoxycarbonyl)phenylmethyl dithiobenzoate (MCPDB).

Phenylmagnesium bromide (0.60 g, 3.3 mmol) and 5 mL THF were added into a Schlenk tube under nitrogen protection. The solution was heated to 40 ℃ and carbon disulfide (0.25 g, 3.3 mmol) was added dropwise over 30 minutes. Methyl α-bromophenylacetate (0.77 g, 3.4 mmol) was then added, and the solution was heated to 80 ℃ and refluxed for 24 hours under nitrogen protection. After that, ice water was added to stop reaction, and the solution was extracted with 3 × 15 mL diethyl ether. The combined diethyl ether layers were dried with anhydrous sodium sulfate overnight. After filtration and removal of diethyl ether by rotatory evaporation, column chromatography on silica gel (particle size, 0.035-0.070 mm) with the eluent (hexanes : diethyl ether (9:1)), and drying in a vacuum oven overnight, afforded an orange-red oil (0.91 g, yield 91.6%). ^{1}H NMR (300 MHz, $CDCl_3$): δ 8.00 (2H, d, J = 7.4 Hz, S=C(Ar-H)S-), 7.34-7.57 (8H, m, Ar-H), 5.72 (1H, s, -S(Ar)CH-CO-), 3.77 (3H, s, -O-CH_3).

Typical preparation of polystyrene RAFT macro chain transfer agent (mCTA)[36]

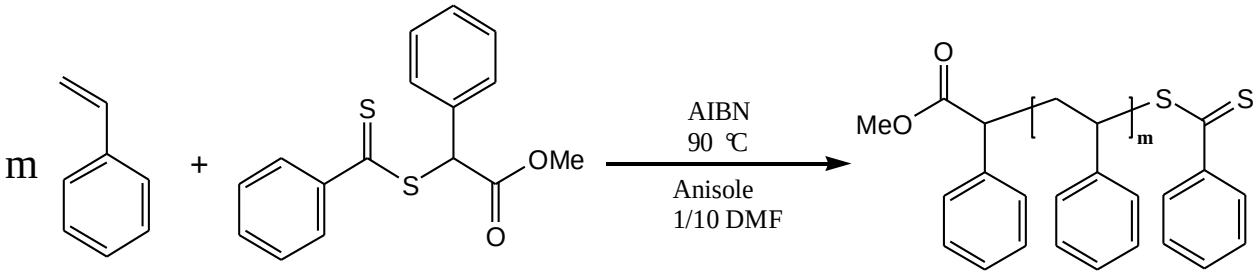

Figure 10. Synthesis of polystyrene RAFT mCTA.

In a typical RAFT reaction (PS_{40}-mCTA), styrene (21.76 g, 0.21 mol), *S*-α-(Methoxycarbonyl)phenylmethyl dithiobenzoate (MCPDB, 0.63 g, 2.1 mmol), and *2*,*2*-Azobisisobutyronitrile (AIBN, 0.034 g, 0.21 mmol) were dissolved in 10.1 mL anisole with 1.1 mL *N*,*N*-dimethylformamide (DMF) as an internal NMR standard in a Schlenk tube. The Schlenk tube was degassed by three freeze-pump-thaw cycles and refilled with nitrogen. After the freeze-pump-thaw cycles, a small amount (~0.2 mL) of the initial mixture was taken out for ^{1}H NMR analysis, and the result was applied as "0%" conversion for the future monitoring and calculation of reaction conversion. The mixture was then heated to 90 ℃ for 141 hours. To monitor conversion over time, a small volume (~0.2 mL) of mixture was periodically carefully taken out from the Schlenk tube by a nitrogen-filled syringe. The reaction was ended when the desired conversion (60%) was reached by ^{1}H NMR monitoring. The solution was re-precipitated twice into methanol (50 mL each) and dried under vacuum oven overnight to get a fine white powder (12.90 g, 94.3% yield based on 60% conversion). ^{1}H NMR (300 MHz, $CDCl_3$): δ 7.8 (2H, m, S=C(Ar-H)S-), 6.4-7.3 (br, 5H per unit of PS, Ar-H), 1.4-2.2 (br, 3H per unit of PS, -CH_2-CH-). GPC: M_n = 4200, M_w/M_n = 1.3.

Typical preparation of polystyrene-*block*-poly(4-(phenylethynyl)styrene) (PS-*b*-PPES) diblock copolymers by RAFT[37]

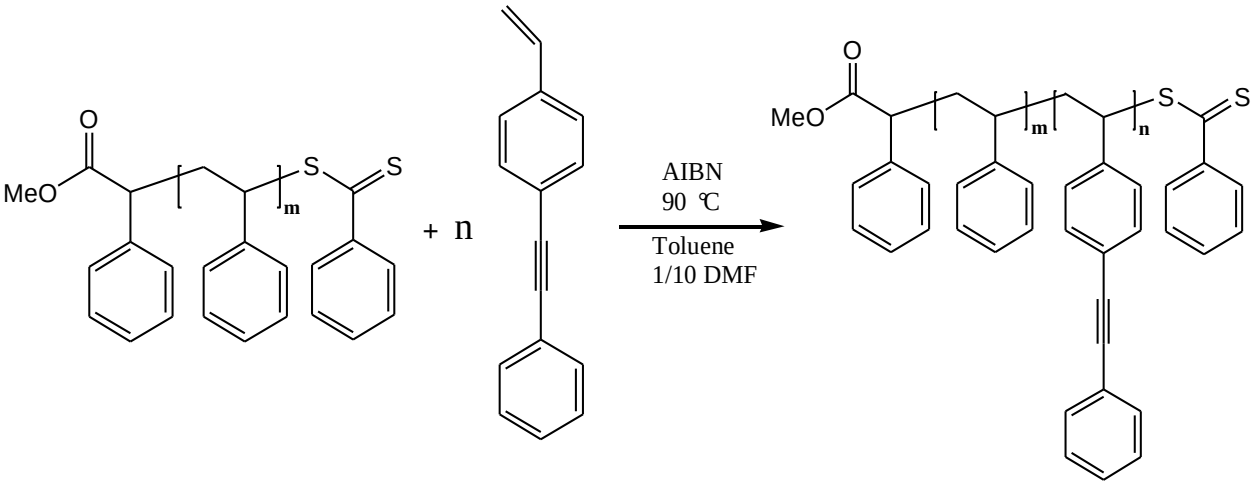

Figure 11. Synthesis of PS-*b*-PPES diblock copolymers by RAFT.

In a typical RAFT reaction (for PS_{40}-$PPES_{20}$), the PS_{40}-mCTA (0.40 g, 0.095 mmol), 4-PES (0.80 g, 3.92 mmol), and *2*,*2*-azobisisobutyronitrile (AIBN, 1.56 mg, 0.0095 mmol) were dissolved in 2.2 mL toluene with 0.24 mL *N*,*N*-dimethylformamide (DMF) as an internal NMR standard in a Schlenk tube. The Schlenk tube was degassed by three freeze-pump-thaw cycles and refilled with nitrogen. The mixture was then heated to 90 ℃ and stirred for 48 hours (50 % conversion by ^{1}H NMR). The block copolymers were isolated by precipitating with methanol (50 mL each) twice and dried under vacuum oven overnight to afford a pale pink powder (0.7670 g, 95.1% yield based on 50% conversion). ^{1}H NMR (300 MHz, $CDCl_3$): δ 6.4-7.5 (br, 5H per unit of styrene and 9H per unit of 4-PES, Ar-H), 1.4-1.9 (br, 3H per unit of styrene and 3H per unit of 4-PES, -CH_2-CH-). GPC: M_n = 8300, M_w/M_n = 1.4.

Typical preparation of cobalt-copolymer adduct by the addition of cobalt carbonyl to PPES block[37]

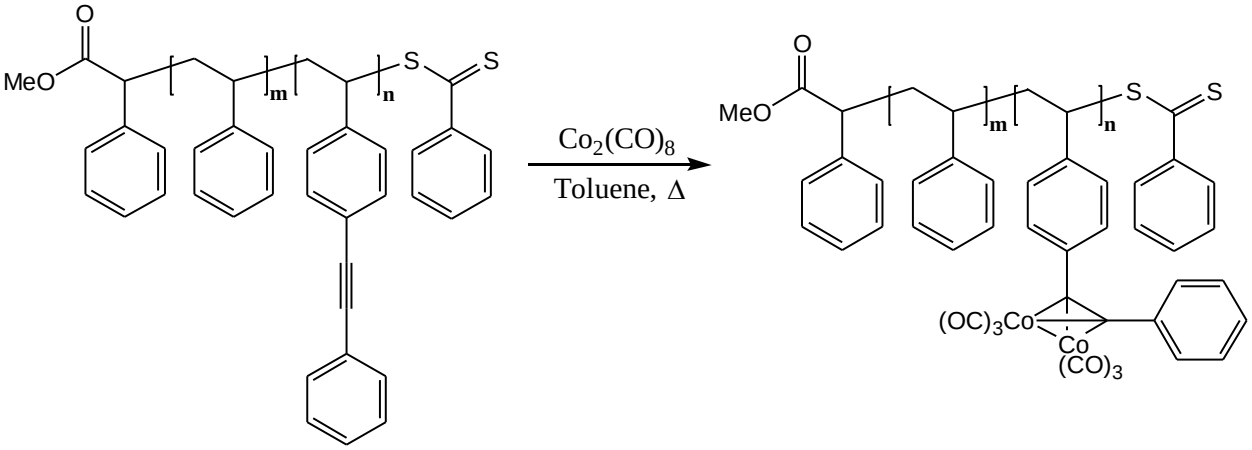

Figure 12. Synthesis of cobalt-polymer adduct by the addition of cobalt carbonyl to PPES block.

In a typical procedure, PS_{40}-$PPES_{20}$ (0.3 g, 36.1 μmol, 0.72 mmol PES units, M_n (NMR) = 8.3 kg/mol, M_w/M_n = 1.4) and $Co_2(CO)_8$ (0.25 g, 0.73 mmol, 1 equiv of $Co_2(CO)_8$ added per PES repeat unit) were dissolved in anhydrous toluene (10 mL) in a glovebox. The mixture was stirred 24 hours under nitrogen and precipitated twice into methanol (50 mL each) to afford desired product PS_{40}-$PPES_{20}[Co_2(CO)_6]_{18}$ as a dark-brown powder. Here, the fraction of alkyne groups converted to dicobalt adducts was estimated as 90%,[37] and the molecular weight fraction of PS block over Co-copolymer adduct PS_m-$PPES_n[Co_2(CO)_6]_x$ is calculated as equation (3):

$$f_{PS} = \frac{MW_{Styrene} \times m}{MW_{Styrene} \times m + MW_{4-PES} \times n + MW_{[Co_2(CO)_6]} \times x} \qquad (3)$$

Where m, n, and x represents the repeat units of each component. So, f_{PS} = 0.31 for PS_{40}-$PPES_{20}[Co_2(CO)_6]_{18}$. The product was stored in the freezer. ^{1}H NMR (300 MHz, $CDCl_3$): δ 6.4-7.5 (br, 5H per unit of styrene and 9H per unit of 4-PES, Ar-H), 1.2-1.9 (br, 3H per unit of styrene and 3H per unit of 4-PES, -CH_2-CH-).

TEM sample preparation[37]

The PS_m-$PPES_n[Co_2(CO)_6]_x$ samples were dissolved in toluene (5–10 mg/mL). The solution was drop-cast onto a carbon-coated copper grid in a N_2-filled glovebox. The solvent was evaporated overnight at room temperature.

Results and Discussion

RAFT macro chain transfer agent (mCTA)

A series of styrene-based macro chain transfer agents (mCTA) were synthesized by reversible addition-fragmentation chain transfer (RAFT) polymerization. *S*-α-(Methoxycarbonyl)phenylmethyl dithiobenzoate (MCPDB) was chosen as chain transfer agent (CTA) because of its high efficiency[36] to control the living radical polymerization of a wide range of vinyl monomers such as styrene. In addition, the polymers could be synthesized with predictable M_n, high conversion and low polydispersity. The reaction was carried out at 90 ℃ in toluene and *N*,*N*-dimethylformamide (DMF) with volume ratio as 10 : 1, where DMF acts as an internal standard to monitor conversion by ^{1}H NMR (Figure A7 and A8). Conversion was calculated as equation (A1) in appendix. Results of these mCTAs are shown in Table 1.

Table 1. Results for PS-mCTA by RAFT

[a]mCTAs	Time (hours)	Temperature (℃)	[b]Conversion (%)	M_n by conversion (g/mol)	[c]M_n by GPC (g/mol)	[d]M_w/M_n
PS_{17}-mCTA	88	90	49	2600	1800	1.32
PS_{40}-mCTA	141	90	60	6200	4200	1.34
PS_{89}-mCTA	88	90	52	10900	9300	1.25
PS_{125}-mCTA	88	90	45	14000	13000	1.27

[a]Macro chain transfer agent (mCTA)a composition was calculated from [c]M_n by GPC. [b]Conversion was calculated from ^{1}H NMR spectra by comparison of styrene signals. [d]M_w/M_n was also characterized by GPC.

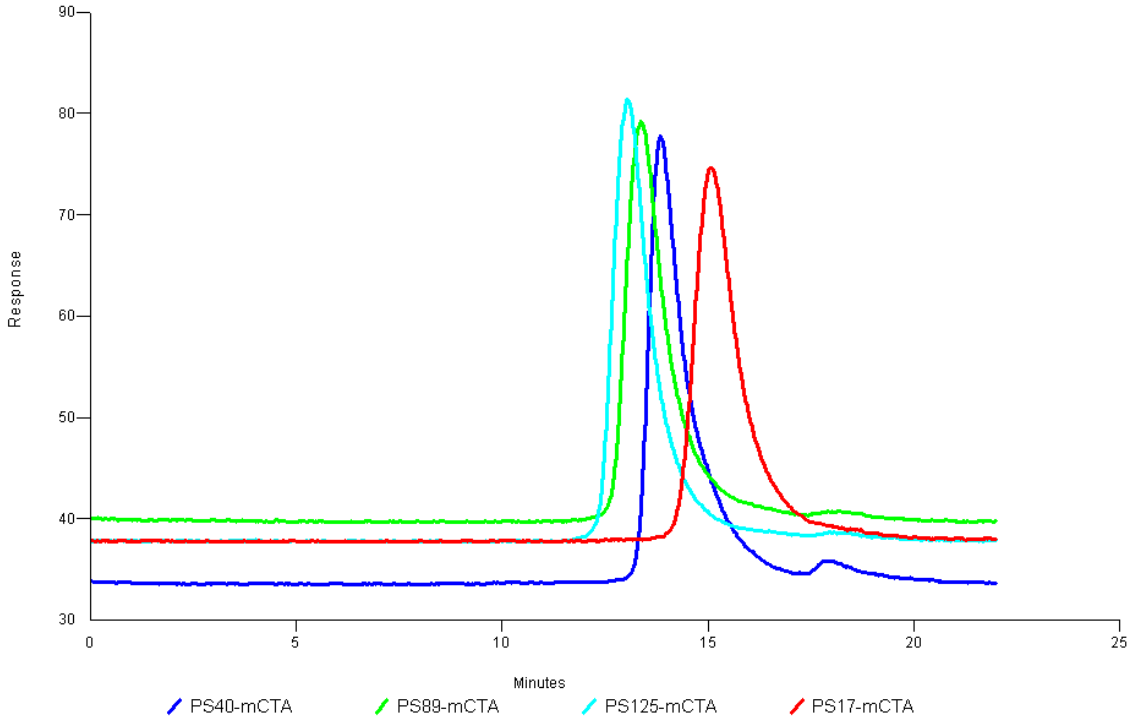

Figure 13. GPC profiles for macro chain transfer agents (mCTAs): PS_{17}-mCTA (red), PS_{40}-mCTA (dark-blue), PS_{89}-mCTA (green), PS_{125}-mCTA (blue).

Here, we synthesized a series of PS-mCTA ranging from 1800 g/mol to 13000 g/mol based on GPC results. All the homopolymerizations result in a relatively low polydispersity index (~1.3) and the M_w/M_n values do not change so much with increasing molecular weight. Because the GPC standard for our characterization is polystyrene which is very similar to PS-mCTA, we would prefer to follow the GPC's results for the calculation of PS-mCTA composition. The end groups were preserved for future preparation of diblock copolymers by RAFT polymerization, because there is no PS-mCTA signal in the GPC profiles of the diblock copolymers (Figure 14). Figure 13 shows the shift of mCTAs with different molecular weight of polystyrene block.

Polystyrene-*block*-poly(4-(phenylethynyl)styrene) (PS-*b*-PPES) diblock copolymers

A series of polystyrene-*block*-poly(4-(phenylethynyl)styrene) (PS-*b*-PPES) diblock copolymers were synthesized by RAFT polymerization of PES from PS-mCTAs. Each mCTA was polymerized with 4-PES with to afford PS-*b*-PPES diblock copolymers at 5 different PS/PPES ratios in order to form different morphologies after self-assembly. The RAFT polymerizations were performed at 90 ℃ in toluene with DMF as an internal standard for monitoring conversion by ^{1}H NMR. Figure A9 and A10 show the comparative ^{1}H NMR spectra for monitoring conversion during the synthesis of PS_{40}-$PPES_{20}$. Conversion was calculated in the same formula as equation (1A) which only changed the styrene to 4-PES.

Compositions, conversions, molecular weights, and GPC results of these diblock copolymers are shown in Table 2. The molecular weight distribution of the diblock copolymers was broader than that of the parent mCTA, ranging from 1.30 to 1.72. When the molecular weight of PPES block was below 10 kg/mol, the observed M_w/M_n was lower than 1.5. However, the M_w/M_n increased (> 1.5) as the PPES block got longer (M_n > 10 kg/mol).

Table 2. Results for PS-*b*-PPES diblock copolymers by RAFT

[a]Copolymers	Time (hours)	Temperature (℃)	[b]Conversion (%)	[c]M_n by conversion (g/mol)	M_n by GPC (g/mol)	[d]M_w/M_n
PS_{17}-$PPES_8$	31	90	73	3400	3400	1.48
PS_{17}-$PPES_{19}$	32	90	63	5600	5200	1.43
PS_{17}-$PPES_{28}$	65	90	55	7600	6500	1.37
PS_{17}-$PPES_{30}$	65	90	59	7900	8700	1.41
PS_{17}-$PPES_{46}$	49	90	52	11200	9100	1.45
PS_{40}-$PPES_{11}$	38	90	45	6500	6700	1.34
PS_{40}-$PPES_{20}$	38	90	48	8300	8300	1.39
PS_{40}-$PPES_{32}$	48	90	55	10700	9400	1.40
PS_{40}-$PPES_{39}$	55	90	46	12100	9900	1.53
PS_{40}-$PPES_{74}$	102	90	45	19400	12400	1.66
PS_{89}-$PPES_9$	24	90	78	11200	10500	1.32
PS_{89}-$PPES_{23}$	42	90	56	14000	12700	1.32
PS_{89}-$PPES_{41}$	75	90	62	17600	14200	1.48
PS_{89}-$PPES_{67}$	75	90	68	22900	15900	1.62
PS_{89}-$PPES_{89}$	45	90	69	27500	16100	1.56
PS_{125}-$PPES_{12}$	29	90	70	15500	13200	1.30
PS_{125}-$PPES_{25}$	65	90	55	18100	14500	1.45
PS_{125}-$PPES_{51}$	65	90	56	23500	18800	1.54
PS_{125}-$PPES_{95}$	133	90	50	32400	19000	1.65
PS_{125}-$PPES_{125}$	133	90	49	38600	19900	1.72

[a]Diblock copolymer composition was calculated from [c]M_n by conversion. [b]Conversion was calculated from ^{1}H NMR spectra by comparison of styrene signals. [d]M_w/M_n was also characterized by GPC.

Here, we apply the M_n measured by conversion (^{1}H NMR) to calculate the diblock copolymer composition for two reasons. First, GPC was inaccurate for the analysis of these polymers because the standards used to calibrate the GPC are polystyrene which is quite different from the PPES blocks in our copolymers. So the GPC results show great deviation from M_n by conversion when PPES block gets longer. However, GPC was still useful for monitoring relative changes in molecular weight and estimating the molecular weight distribution of these diblock copolymers. Second, in the ^{1}H NMR spectra (Figure A5, A9, A10), the aromatic PS and PPES signals overlap with the solvent peak for *d*-chloroform and the alkyl PS and PPES signals

overlap with water peak. So we could not directly calculate the copolymer molecular weight from the ^{1}H NMR spectra. As a result, we put the conversion results in equation (4) to calculate the molecular weight of the diblock copolymers.

$$\boldsymbol{M_{n,\ theoretical}} = \frac{[\boldsymbol{4-PES}]_0 \times \boldsymbol{MW_{4-PES}} \times \boldsymbol{p}}{[\boldsymbol{mCTA}]_0} + \boldsymbol{MW_{mCTA}} \qquad (4)$$

Where $[4\text{-PES}]_0$ is the initial concentration of monomer 4-PES, $MW_{4\text{-PES}}$ is the molecular weight of 4-PES, p is the conversion measured by ^{1}H NMR, MW_{mCTA} is the molecular weight of the PS-mCTA, and $[mCTA]_0$ is the initial concentration of PS-mCTA. Figure 14 shows the shift of a typical PS_{17}-*b*-PPES series. The others were shown in appendix (Figure A11, A12, A13).

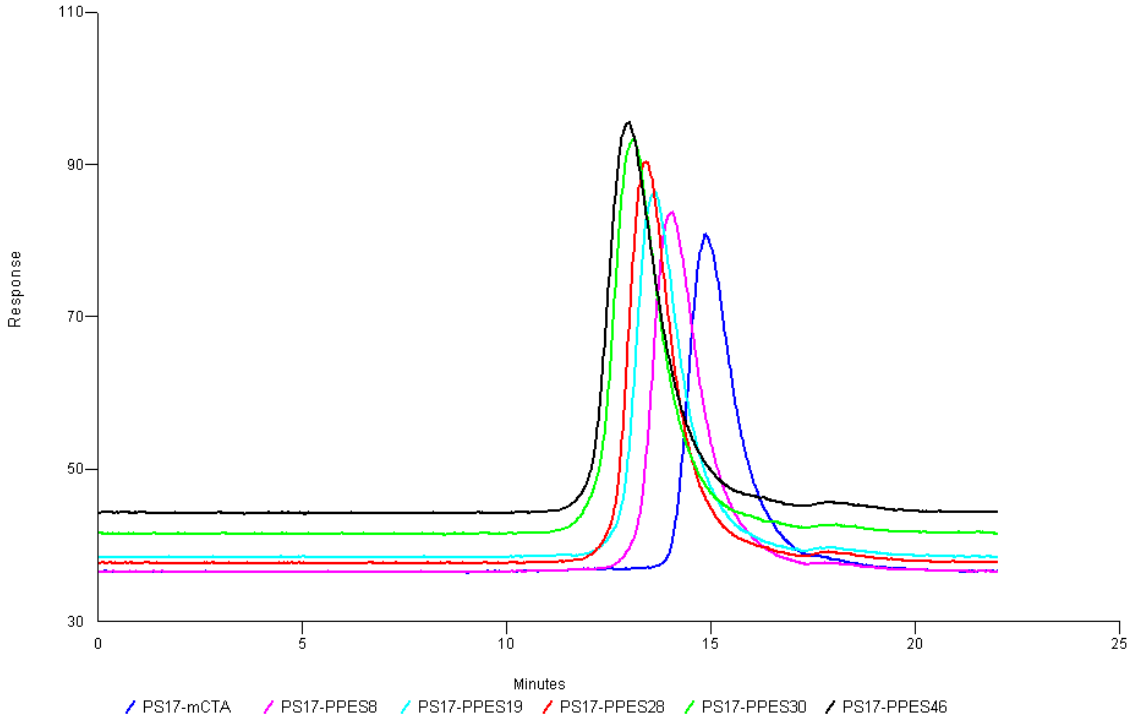

Figure 14. GPC profiles for PS-*b*-PPES copolymers, PS_{17} series with its parent mCTA: PS_{17}-mCTA (dark-blue), PS_{17}-$PPES_8$ (pink), PS_{17}-$PPES_{19}$ (blue), PS_{17}-$PPES_{28}$ (red), PS_{17}-$PPES_{30}$ (green), PS_{17}-$PPES_{46}$ (black).

Thermoanalysis for diblock copolymers and Co-copolymer adducts

DSC measurements were carried out with heating scan rate as 10 ℃/min from 0 to 200 ℃ for all diblock copolymers. The diblock copolymer sample were sequentially scanned for two cycles (heated from 0 ℃ to 200 ℃, then cooled down to 0 ℃, reheated to 200 ℃ again, last cooled down to 0 ℃). The onset of the T_g was measured from second heating scan. A typical DSC profile for PS_{40}-$PPES_{20}$ (M_n = 8.3 kg/mol; 49 wt % PPES, T_g = 109 ℃) copolymer is shown in Figure 15.

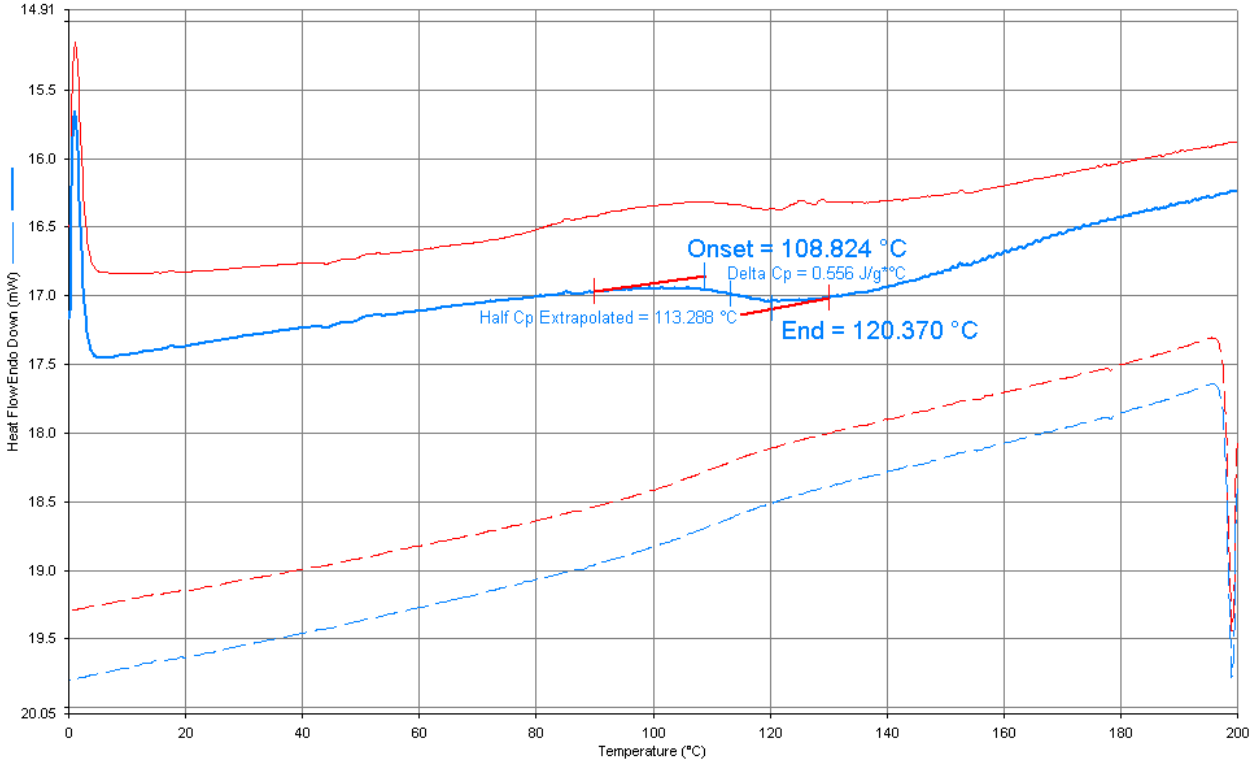

Figure 15. DSC profile for PS_{40}-$PPES_{20}$ diblock copolymer, first cycle (red lines) and second cycle (blue lines), heated from 0 ℃ to 200 ℃ (solid lines) and cooled from 200 ℃ to 0 ℃ (dash lines), the onset glass transition temperature (T_g) measured from second heating scan.

The second heating scans of diblock copolymers (Table 3) with different compositions were chosen in Figure 16 to further confirm the miscibility of PPES with PS.

Table 3. Diblock copolymers for DSC characterization

Copolymers	M_n (kg/mol)	[a]wt % PPES	[b]T_g (℃)
PS_{125}-$PPES_{12}$	15.5	16	96
PS_{40}-$PPES_{11}$	6.5	35	102
PS_{40}-$PPES_{20}$	8.3	49	110
PS_{40}-$PPES_{39}$	12.1	65	122
PS_{17}-$PPES_{46}$	11.2	84	129

[a]wt % PPES is the molecular weight percentage of PPES block over diblock copolymer. [b]T_g is the onset glass transition temperature from DSC profile (second heating scan).

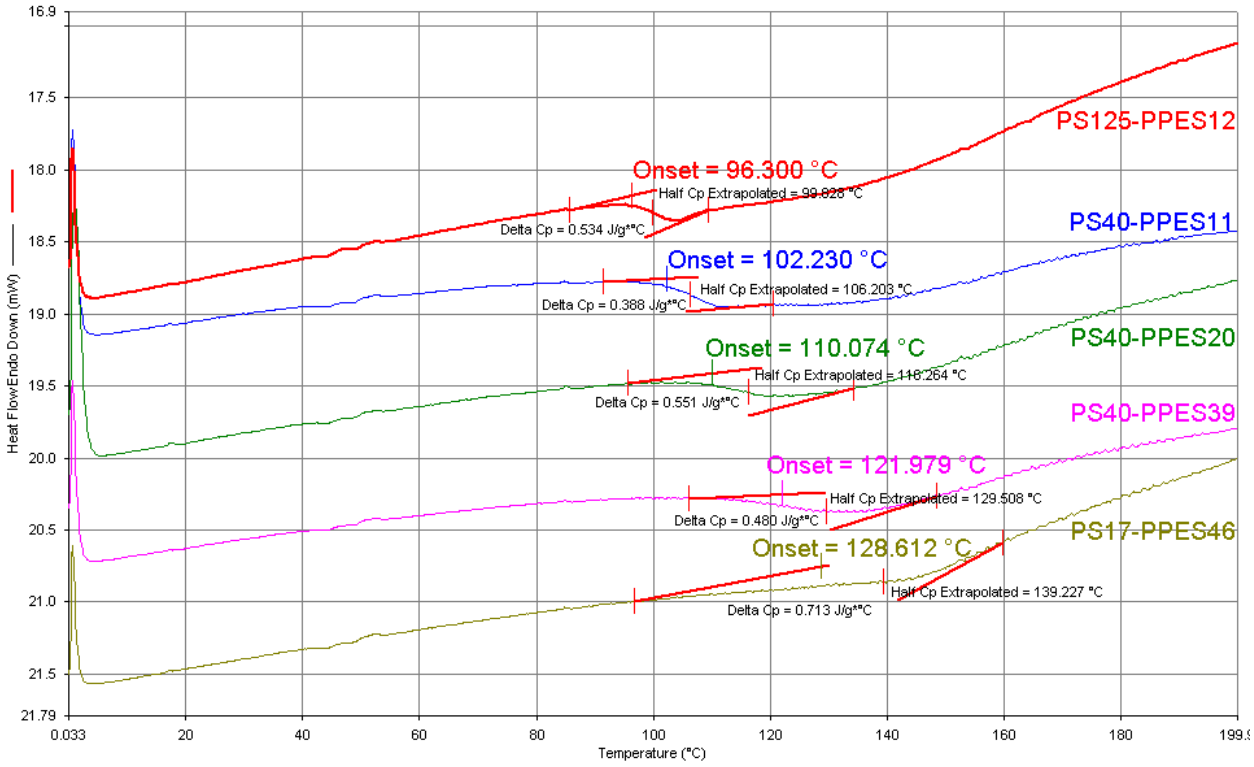

Figure 16. Comparative DSC profiles (second heating scan) for diblock copolymers

The onset T_g of these diblock copolymers increases with the increasing molecular weight percentage of PPES block. In addition, the DSC profiles showed a single glass transition can prove a complete miscibility of two PPES and PS blocks in diblock copolymers.

Then the reported T_g[18] of PS (T_g = 92 ℃) and PPES (T_g = 154 ℃) was substituted into Fox equation (5) to calculate the T_g of diblock copolymers:

$$\frac{1}{T_g} = \frac{w_1}{T_{g,1}} + \frac{w_2}{T_{g,2}} \qquad (5)$$

Where $T_{g,1}$ and $T_{g,2}$ is the glass transition temperature of PS block and PPES block, w_1 and w_2 are weight fractions of PS block and PPES block. The T_g, calculated from Fox equation (shown in Table 4) of diblock copolymers was consistent with $T_{g,\text{half Cp}}$ (Figure 16), however further studies to control for molecular weight effects on the T_g of PS and PPES will be necessary.

Table 4. DSC results for diblock copolymer from Fox equation

Copolymers	w_1	w_2	[a]T_g (℃)	[b]$T_{g,\text{half Cp}}$ (℃)
PS_{125}-$PPES_{12}$	0.84	0.16	98	100
PS_{40}-$PPES_{11}$	0.65	0.35	107	106
PS_{40}-$PPES_{20}$	0.51	0.49	115	116
PS_{40}-$PPES_{39}$	0.35	0.65	125	129
PS_{17}-$PPES_{46}$	0.16	0.84	139	139

[a]T_g was calculated from Fox equation, [b]$T_{g,\text{half Cp}}$ was measured from Figure 16.

Cobalt-copolymer adducts were synthesized by incorporating 1 equiv $Co_2(CO)_8$ into per PES repeat units in toluene under nitrogen protection. The product was purified by precipitated into methanol. Figure 17 shows the comparison of IR spectra for a typical cobalt-copolymer adduct, PS_{89}-$PPES_{41}[Co_2(CO)_6]_{37}$ before and after heating in bulk at 110 ℃ for 24 hours. The spectra show the disappearance of the signals at 2010, 2048, and 2088 cm^{-1} which represent the CO groups in $Co_2(CO)_6$ adducts. The new peaks from 1400-1600 cm^{-1} possibly result from aromatic C=C from benzene rings and the conjugated C=C which was formed by cross-linking of the alkyne-functional groups in the PPES block after heating.

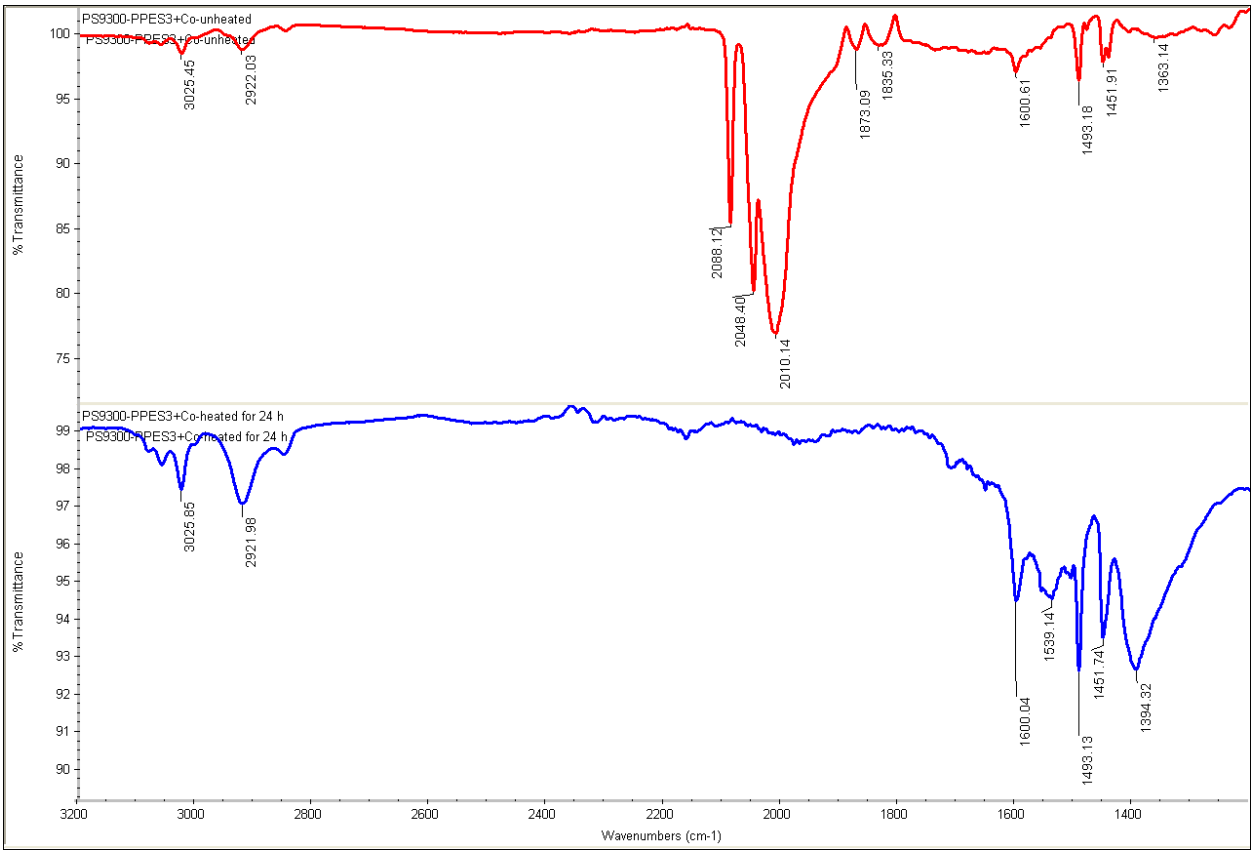

Figure 17. Comparative IR spectrum for Co-copolymer adduct, PS_{89}-$PPES_{41}[Co_2(CO)_6]_{37}$, before (red) and after (blue) being heated at 110 ℃ for 24 hours.

TEM analysis of PS_m-$PPES_n[Co_2(CO)_6]_x$ samples

TEM characterization was carried out to analyze phase separation of the Co-copolymer adducts. TEM samples were prepared by drop-casting PS_m-$PPES_n[Co_2(CO)_6]_x$ samples (dissolved in toluene, 5 –10 mg/mL) onto a carbon-coated copper grid in a N_2-filled glovebox and allowing solvent to evaporate overnight at room temperature. After addition of cobalt to PPES blocks, the PPES blocks appear dark in TEM images, conversely, PS blocks appear as light regions in the TEM images. Four samples (Table 5) were chosen here to compare their micro-phase separation behavior in Figure 18.

Table 5. Cobalt-copolymer adducts for TEM characterization

Cobalt-copolymer adducts	[a]f_{PS}(PS-*b*-PPES)	[b]f_{PS}(PS-*b*-PPES/$Co_2(CO)_6$)	[c]Observed morphology
PS_{89}-$PPES_{23}[Co_2(CO)_6]_{21}$	0.66	0.46	cylindrical
PS_{89}-$PPES_{41}[Co_2(CO)_6]_{37}$	0.53	0.33	cylindrical
PS_{125}-$PPES_{51}[Co_2(CO)_6]_{46}$	0.55	0.35	cylindrical
PS_{125}-$PPES_{125}[Co_2(CO)_6]_{112}$	0.34	0.18	cylindrical

[a]f_{PS}(PS-*b*-PPES) is the molecular weight fraction of PS block over diblock copolymer without cobalt complex, [b]f_{PS}(PS-*b*-PPES/$Co_2(CO)_6$) is molecular weight fraction of PS block over cobalt-copolymer adduct. [c]Observed morphology is tentative which need to be further confirmed by SAXS.

All of the four samples appear to form cylindrical morphologies. Comparison of PS_{89}-$PPES_{41}[Co_2(CO)_6]_{37}$ and PS_{125}-$PPES_{51}[Co_2(CO)_6]_{46}$ (Figure 18 **b** and **c**) shows that the domain sizes of both blocks increase with increasing number of styrene and PES repeat units, and the morphology stays the same if f_{PS}(PS-*b*-PPES/$Co_2(CO)_6$) keeps in constant. In addition, with the constant PS block *dp* = 89 (*dp* is degree of polymerization) but PPES block changed from *dp* = 23 to *dp* = 41 (from Figure 18 **a** to **b**), the chains get longer and the domain size of the PPES block increases. To compare PS_{89}-$PPES_{23}[Co_2(CO)_6]_{21}$ and PS_{125}-$PPES_{125}[Co_2(CO)_6]_{112}$ (Figure 18 **a** and **d**) that both form cylinders but have decreasing f_{PS}(PS-*b*-PPES/$Co_2(CO)_6$) from 0.46 to

0.18, for PS_{89}-$PPES_{23}[Co_2(CO)_6]_{21}$, polystyrene is the majority domain; and for PS_{125}-$PPES_{125}[Co_2(CO)_6]_{112}$, polystyrene is the minority domain. The predictions from TEM images should be further confirmed by small-angle X-ray scattering (SAXS), and more TEM work should be carried to map the relationship between various PS/PPES ratios and the different morphologies of self-assembled cobalt-copolymer adducts.

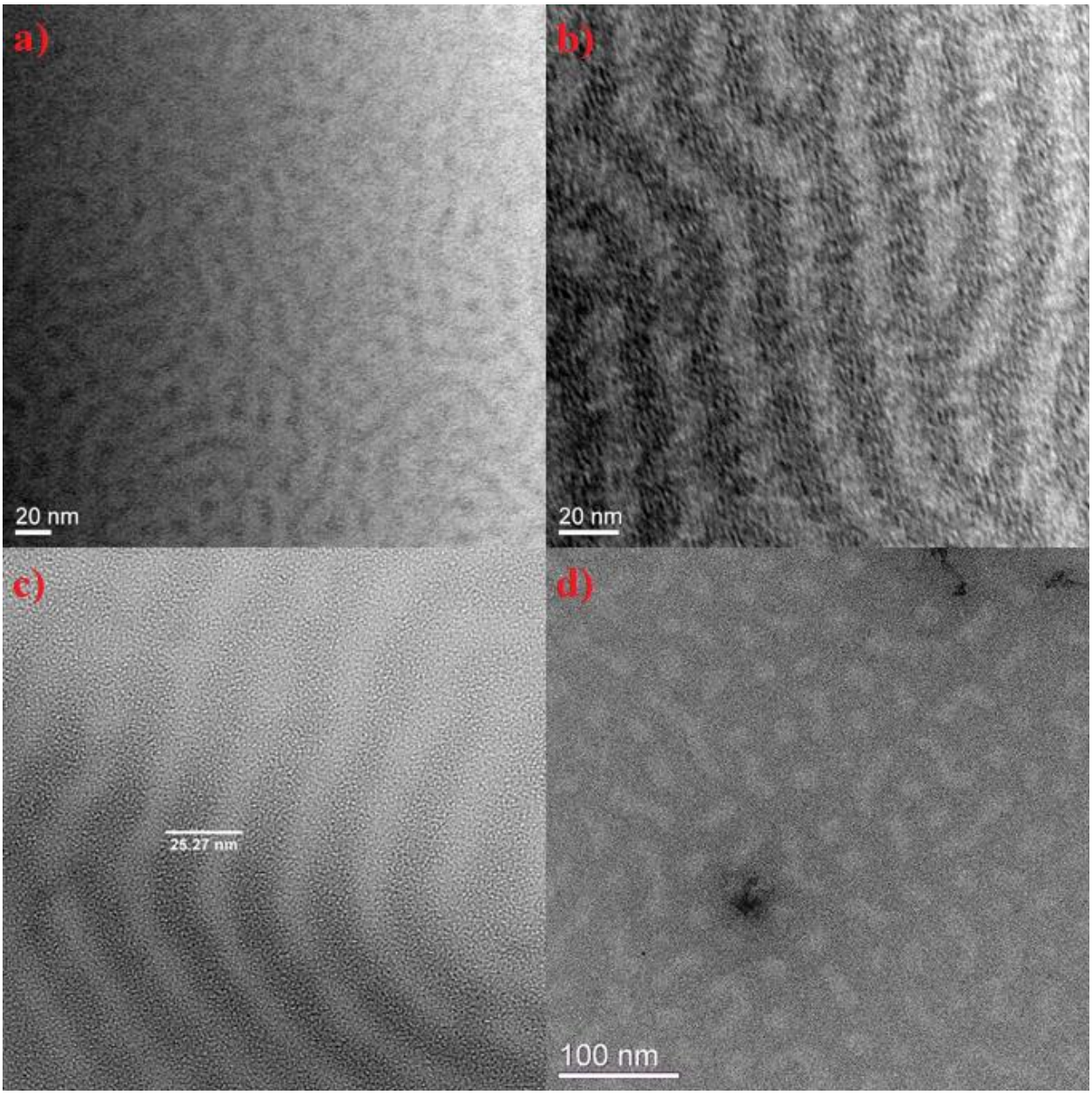

Figure 18. Comparative TEM images for cobalt-copolymer adducts, a) PS_{89}-$PPES_{23}[Co_2(CO)_6]_{21}$, b) PS_{89}-$PPES_{41}[Co_2(CO)_6]_{37}$, c) PS_{125}-$PPES_{51}[Co_2(CO)_6]_{46}$, d) PS_{125}-$PPES_{125}[Co_2(CO)_6]_{112}$.

Conclusions

A series of polystyrene-*block*-poly(4-(phenylethynyl)styrene) (PS-*b*-PPES) diblock copolymers with various PS/PPES ratios was successfully synthesized by RAFT as precursors for cobalt-containing materials which were characterized by ^{1}H NMR and GPC. A complete miscibility for PPES with PS in diblock copolymers was observed by DSC, and loss of CO from cobalt-copolymer adducts was observed by IR spectroscopy after heating in bulk at 110 ℃ for 24 hours. TEM studies were carried out to characterize phase separation of these cobalt-copolymer adducts which appears to form cylindrical morphologies for different compositions (PS_{89}-$PPES_{23}[Co_2(CO)_6]_{21}$, PS_{89}-$PPES_{41}[Co_2(CO)_6]_{37}$, PS_{125}-$PPES_{51}[Co_2(CO)_6]_{46}$, and PS_{125}-$PPES_{125}[Co_2(CO)_6]_{112}$). Increasing the length of PS and PPES blocks leads to an increase in the size of the each domain. In addition, PS_{89}-$PPES_{23}[Co_2(CO)_6]_{21}$ and PS_{125}-$PPES_{125}[Co_2(CO)_6]_{112}$ both form cylinders, but for PS_{89}-$PPES_{23}[Co_2(CO)_6]_{21}$, polystyrene is the majority domain; and for PS_{125}-$PPES_{125}[Co_2(CO)_6]_{112}$, polystyrene is the minority domain. In the future, more TEM and SAXS characterizations should be performed to get a map of the relationship between various PS/PPES ratios and the different morphologies of self-assembled cobalt-copolymer adducts.

References

[1] Ian Manners, *Synthetic Metal-Containing Polymers*; Wiley-VCH: Weinheim, Germany, 2004.

[2] Yasutaka Tsujimoto, Kotaro Satoh, Hidekazu Sugimori, Hiroshi Jinnai, and Masami Kamigaito, *Macromolecules* **2014**, *47*, 944−953.

[3] Liliana A. Mıˆinea, Laura B. Sessions, Kjell D. Ericson, David S. Glueck, and Robert B. Grubbs, *Macromolecules* **2004**, *37*, 8967−8972

[4] Yongping Zha, Raghavendra R. Maddikeri, Samuel P. Gido, Gregory N. Tew, *J Inorg Organomet Polym* **2013**, *23*, 89−94

[5] Robert B. Grubbs, *J. Polym. Sci., Part A: Polym. Chem.* **2005**, *43*, 4323−4336.

[6] Ian Manners, *J. Polym. Sci., Part A: Polym. Chem.* **2002**, *40*, 179−191.

[7] Yiyong Mai, Fan Zhang and Xinliang Feng, *Nanoscale* **2014**, *6*, 106−121

[8] Muruganathan Ramanathan, Yu-Chih Tseng, Katsuhiko Ariga and Seth B. Darling, *J. Mater. Chem. C* **2013**, *1*, 2080−2091.

[9] An-Chang Shi and Baohui Li, *Soft Matter* **2013**, *9*, 1398−1413.

[10] Cheolmin Park, Jongseung Yoon, Edwin L. Thomas, *Polymer* **2003**, *44*, 6725−6760.

[11] Jae-Byum Chang *et al.*, *Nat. Commun.* **5**:3305 **2014**, DOI: 10.1038/ncomms4305.

[12] Scott C. Warren *et al.*, *Science* **320**, 1748 **2008**, DOI: 10.1126/science.1159950.

[13] Hitesh Arora *et al.*, *Science* **330**, 214 **2010**, DOI: 10.1126/science.1193369.

[14] S.B. Darling, *Prog. Polym. Sci.* **2007**, *32*(10), 1152−1204.

[15] M. Christopher Orilall and Ulrich Wiesner, *Chem. Soc. Rev.* **2011**, *40*, 520−535.

[16] Zoltan Mester, Nathaniel A. Lynd, Kris T. Delaney, and Glenn H. Fredrickson, *Macromolecules* **2014**, *47*, 1865−1874.

[17] Meijiao Liu, Weihua Li, and Feng Qiu, *Macromolecules* **2012**, *45*, 9522−9530.

[18] Laura B. Sessions, Liliana A. Mıˆinea, Kjell D. Ericson, David S. Glueck, and Robert B. Grubbs, *Macromolecules* **2005**, *38*, 2116−2121.

[19] Ulrich Mansfeld, Christian Pietsch, Richard Hoogenboom, C. Remzi Becer and Ulrich S. Schubert, *Polym. Chem.* **2010**, *1*, 1560−1598.

[20] Makoto Ouchi, Takaya Terashima, and Mitsuo Sawamoto, *Chem. Rev.* **2009**, *109*, 4963−5050.

[21] Krzysztof Matyjaszewski and Jianhui Xia, *Chem. Rev.* **2001**, *101*, 2921−2990.

[22] Rhiannon K. Iha, Karen L. Wooley, Andreas M. Nystro ̈m, Daniel J. Burke, Matthew J. Kade, and Craig J. Hawker, *Chem. Rev.* **2009**, *109*, 5620−5686.

[23] Graeme Moad, Ezio Rizzardo, and San H. Thang, *Aust. J. Chem.* **2005**, *58*, 379−410.

[24] Graeme Moad, Ezio Rizzardo, and San H. Thang, *Aust. J. Chem.* **2006**, *59*, 669−692.

[25] Graeme Moad, Ezio Rizzardo, and San H. Thang, *Aust. J. Chem.* **2009**, *62*, 1402−1472.

[26] Craig J. Hawker, Anton W. Bosman, and Eva Harth, *Chem. Rev.* **2001**, *101*, 3661−3688.

[27] Andrew B. Lowe, Charles L. McCormick, *Prog. Polym. Sci.* **2007**, *32*, 283–351.

[28] Adam W. York, Stacey E. Kirkland, Charles L. McCormick, *Advanced Drug Delivery Reviews* **2008**, *60*, 1018–1036.

[29] Graeme Moad, Ezio Rizzardo, San H. Thang, *Polymer* **2008**, *49*, 1079–1131.

[30] John T. Lai, Debby Filla, and Ronald Shea, *Macromolecules* **2002**, *35*, 6754–6756.

[31] Tommy S.C. Pai, Christopher Barner-Kowollik, Thomas P. Davis, Martina H. Stenzel, *Polymer* **2004**, *45*, 4383–4389.

[32] David B. Thomas, Anthony J. Convertine, Roger D. Hester, Andrew B. Lowe, and Charles L. McCormick, *Macromolecules* **2004**, *37*, 1735–1741.

[33] Charles L. McCormick and Andrew B. Lowe, *Acc. Chem. Res.* **2004**, *37*, 312–325.

[34] Takashi Ishizone, Kenji Sugiyama, Akira Hirao, and Seiichi Nakahama, *Macromolecules* **1993**, *26*, 3009–3018.

[35] Katsuyuki Tsuda, Ken'ichi Tsutsumi, Manabu Yaegashi, Masahiro Miyajima *et al.*, *Polymer Bulletin* **1998**, *40*, 651–658.

[36] Se ́bastien Perrier, Pittaya Takolpuckdee, James Westwood, and David M. Lewis, *Macromolecules* **2004**, *37*, 2709–2717.

[37] Liliana A. Mıˆinea, Laura B. Sessions, Kjell D. Ericson, David S. Glueck, and Robert B. Grubbs, *Macromolecules* **2004**, *37*, 8967–8972.

Appendix

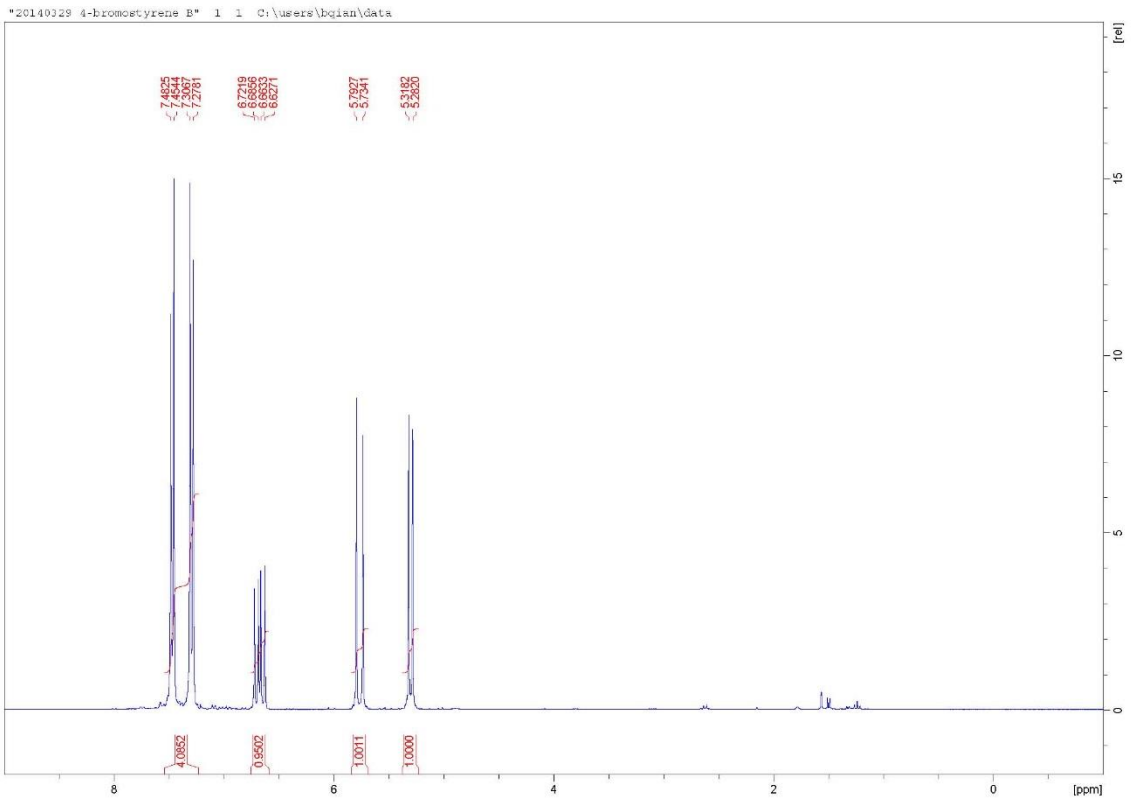

Figure A1. ^{1}H NMR spectrum for 4-bromostyrene.

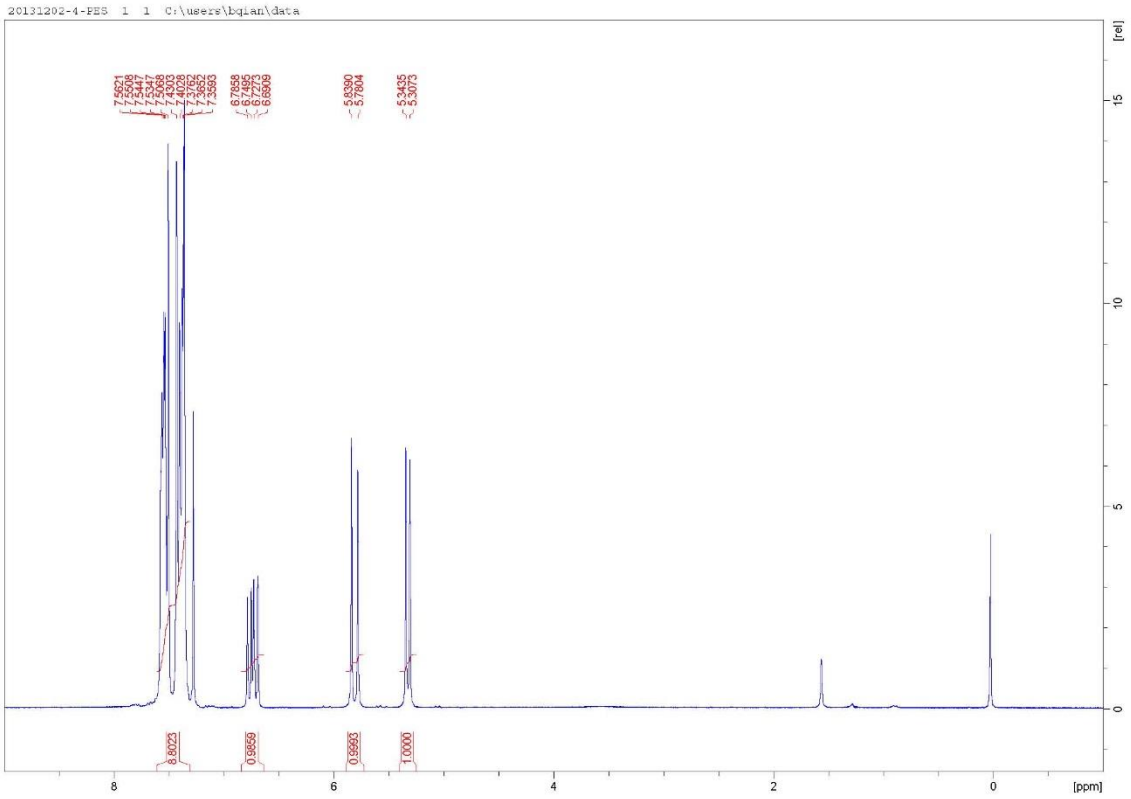

Figure A2. ^{1}H NMR spectrum for 4-(phenylethynyl)styrene (4-PES).

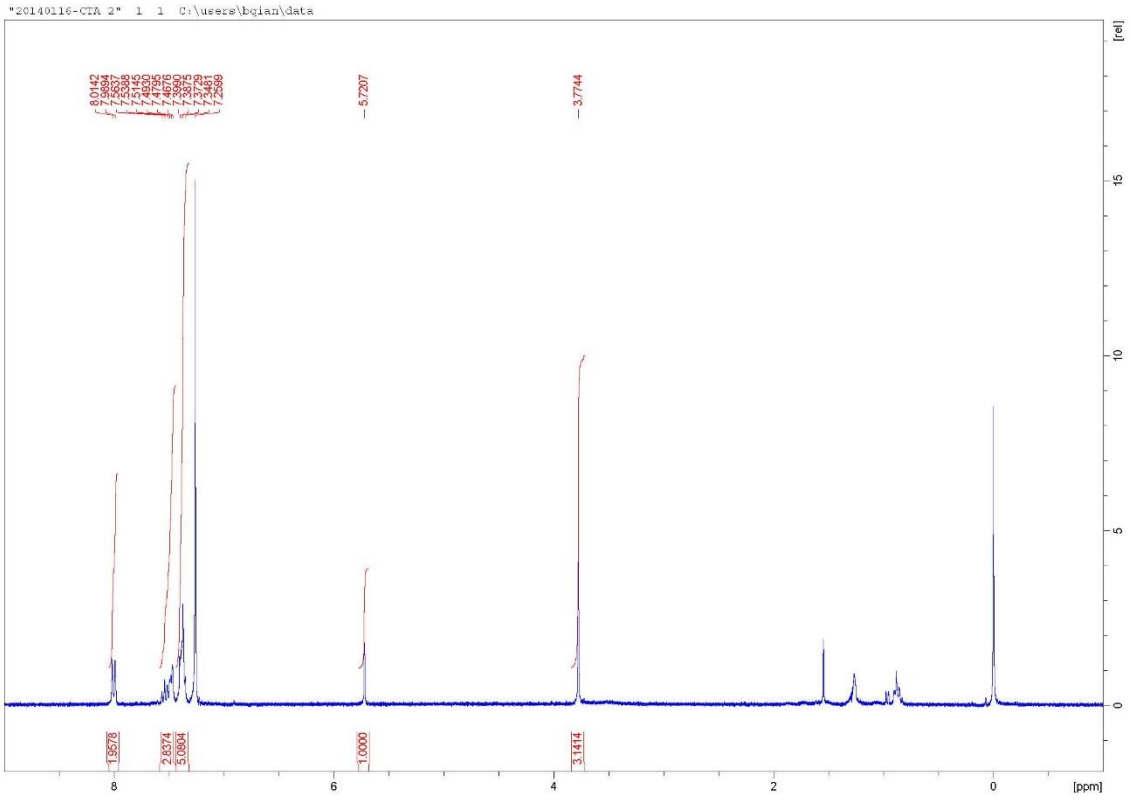

Figure A3. ^{1}H NMR spectrum for chain transfer agent (CTA), MCPDB.

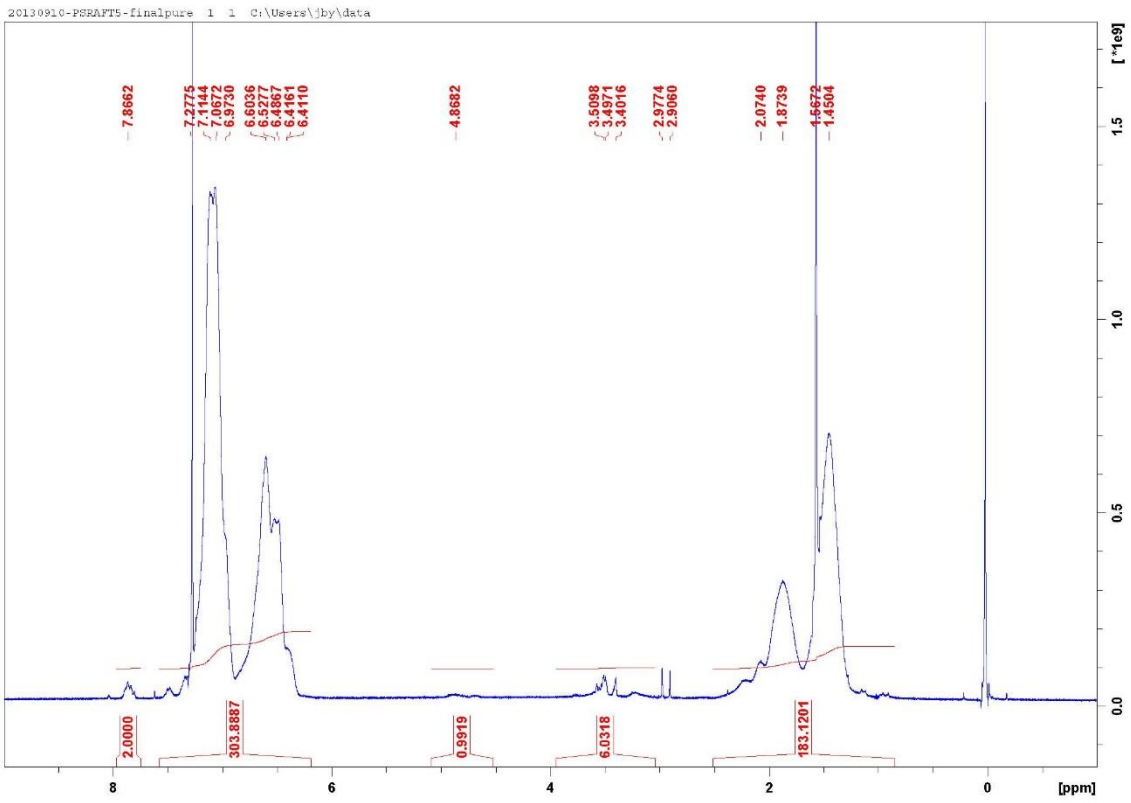

Figure A4. ^{1}H NMR spectrum for macro chain transfer agent (mCTA), PS_{40}-mCTA.

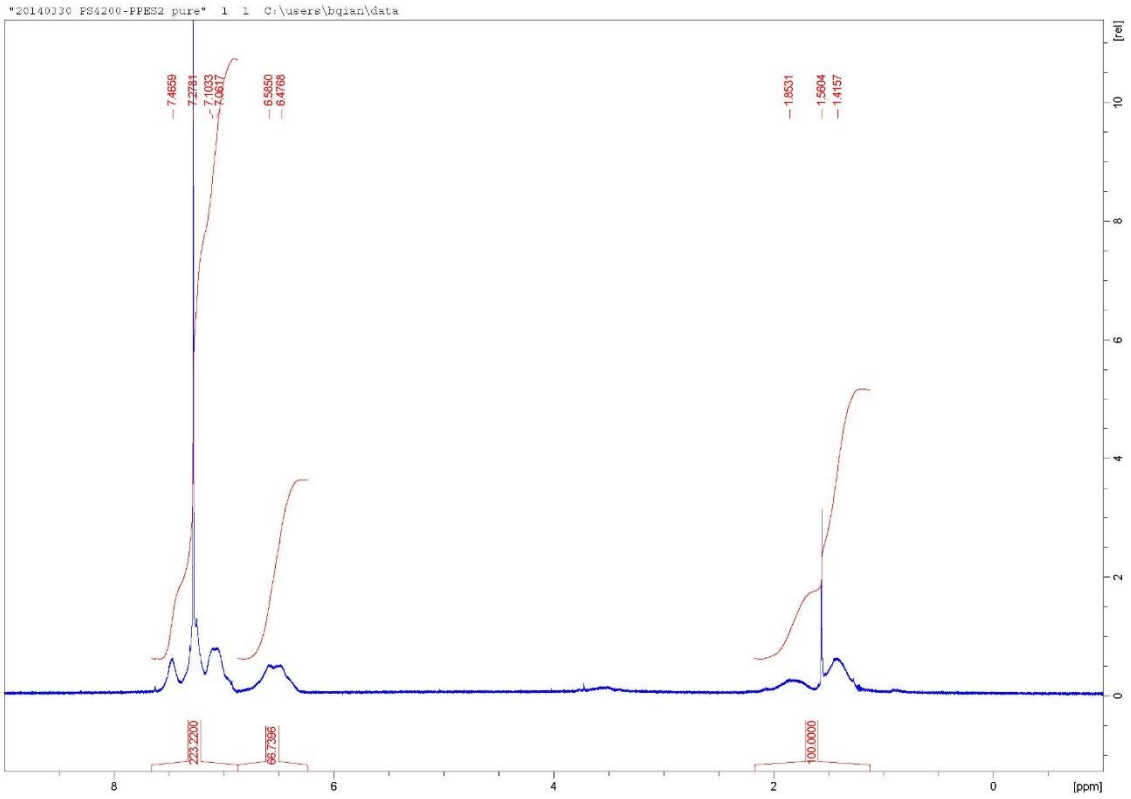

Figure A5. ^{1}H NMR spectrum for polystyrene-*block*-poly(4-(phenylethynyl)styrene) (PS-*b*-PPES) diblock copolymers, PS_{40}-$PPES_{20}$.

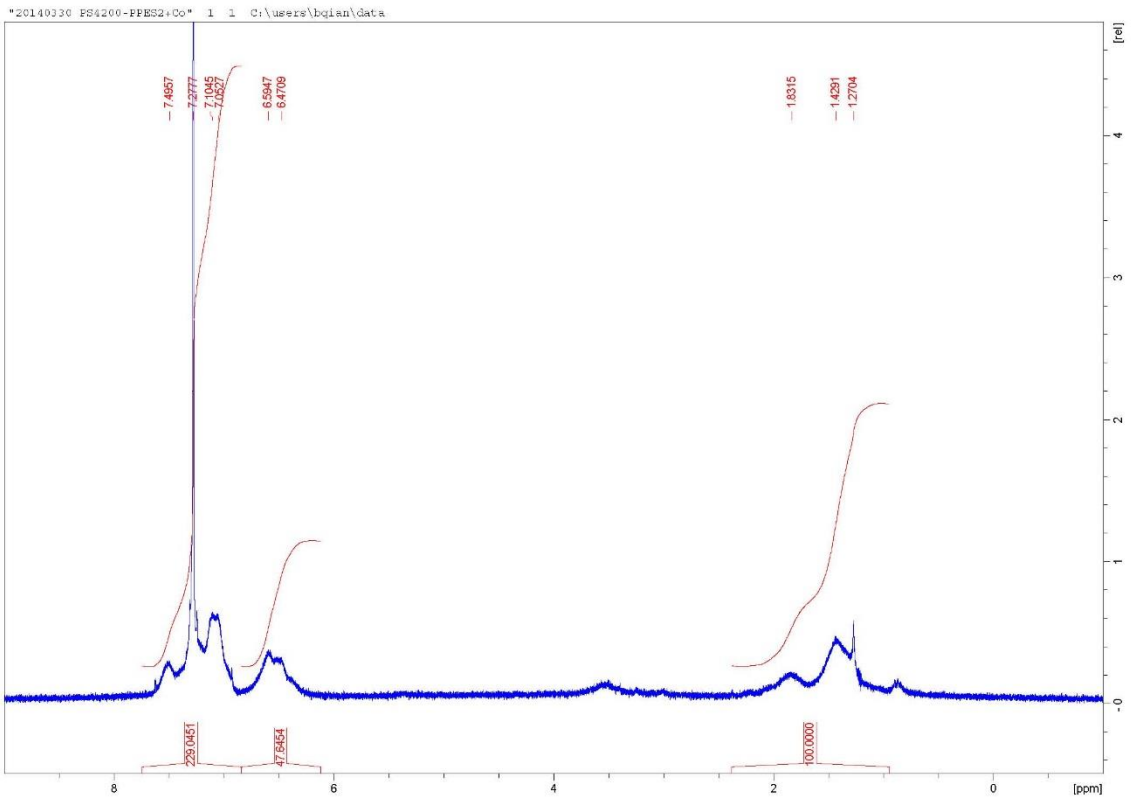

Figure A6. ^{1}H NMR spectrum for Co-copolymer adduct, PS_{40}-$PPES_{20}[Co_2(CO)_6]_{18}$.

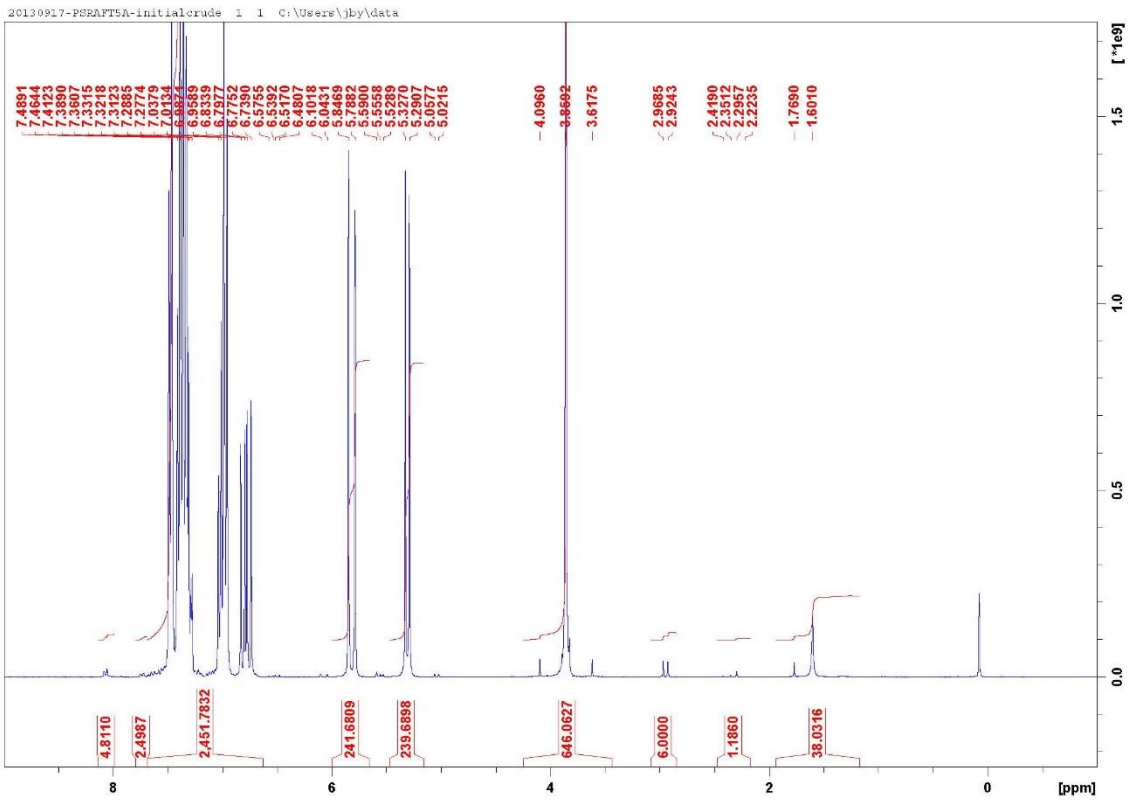

Figure A7. ^{1}H NMR spectrum for PS_{40}-mCTA (initial crude, reaction time = 0 h).

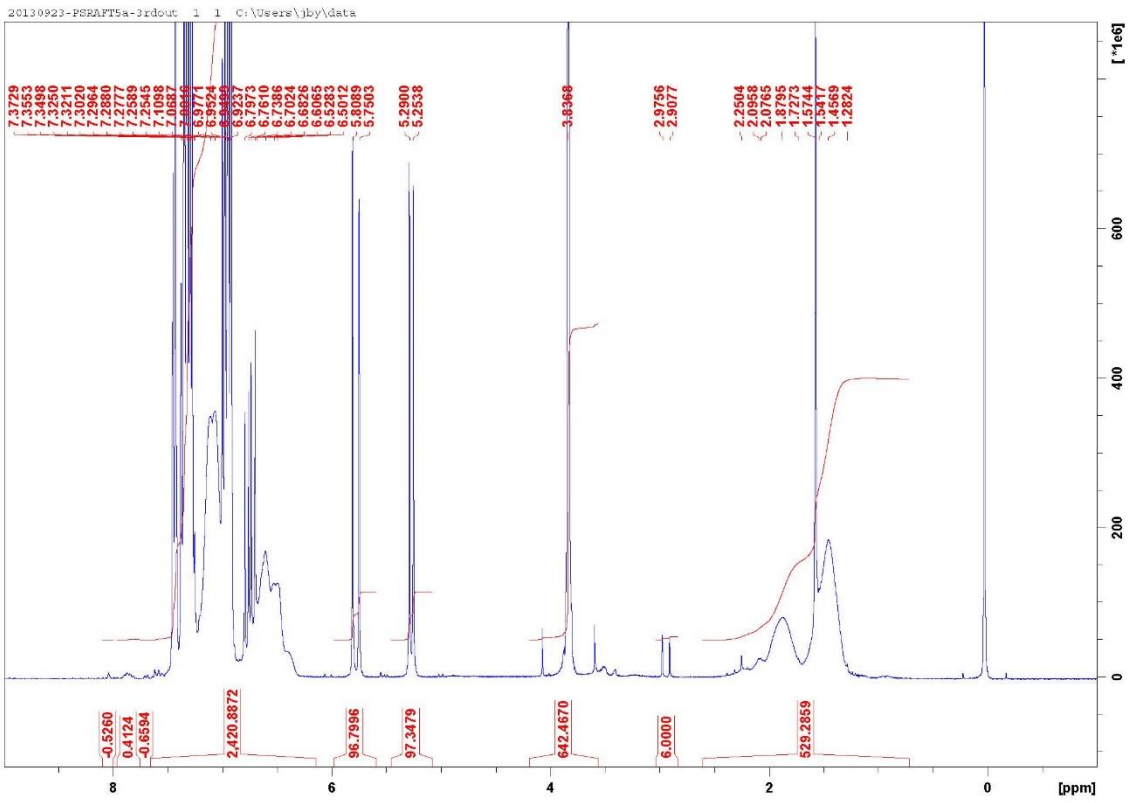

Figure A8. ^{1}H NMR spectrum for PS_{40}-mCTA (final crude, reaction time = 141 h).

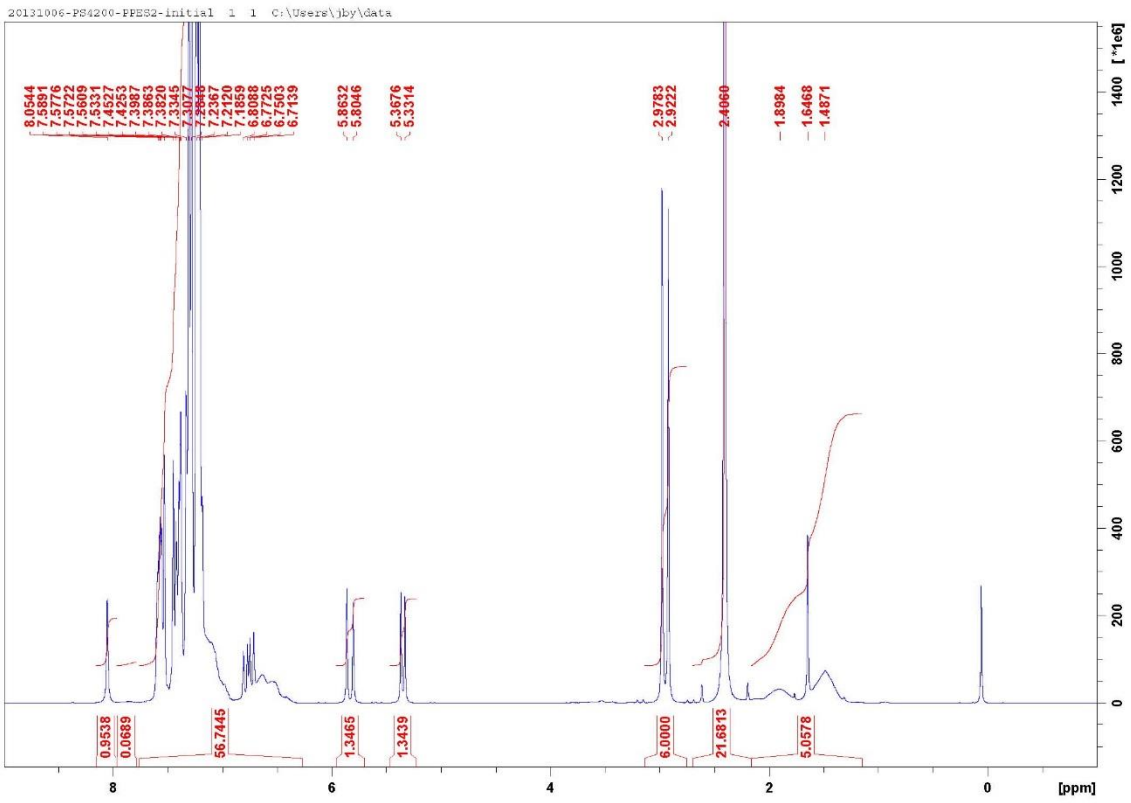

Figure A9. ^{1}H NMR spectrum for PS_{40}-$PPES_{20}$ (initial crude, reaction time = 0 h).

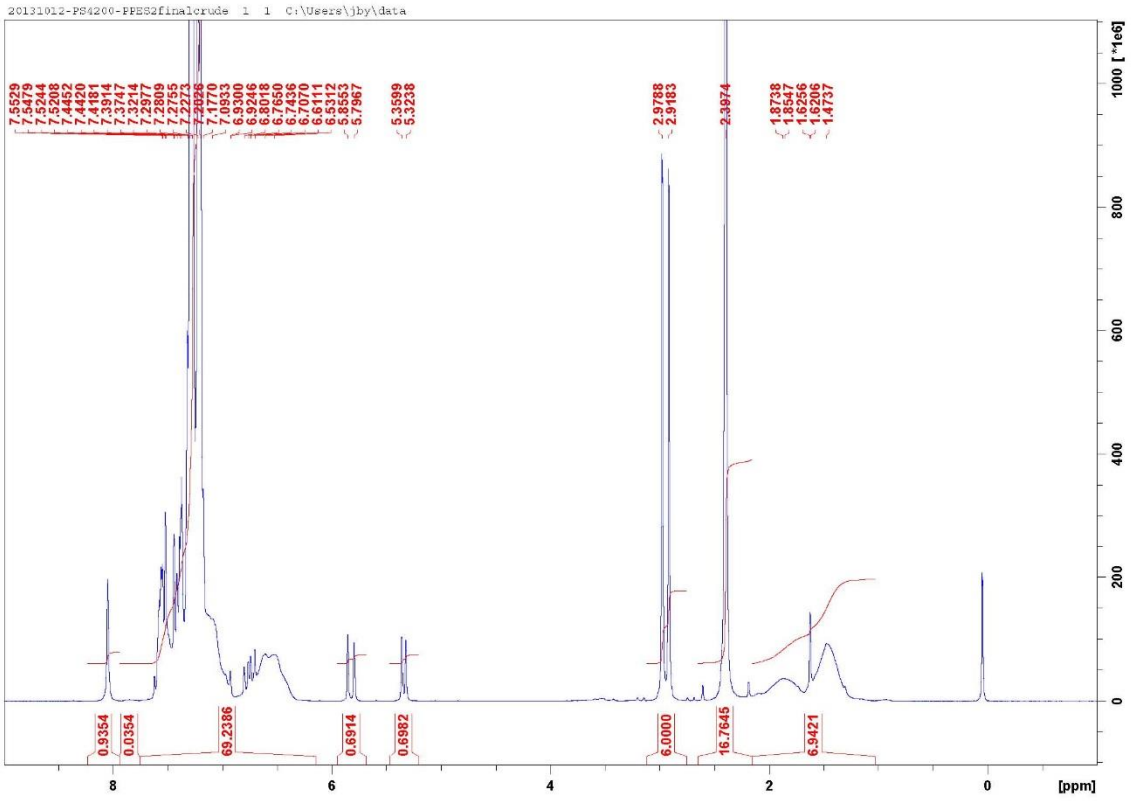

Figure A10. ^{1}H NMR spectrum for PS_{40}-$PPES_{20}$ (final crude, reaction time = 38 h).

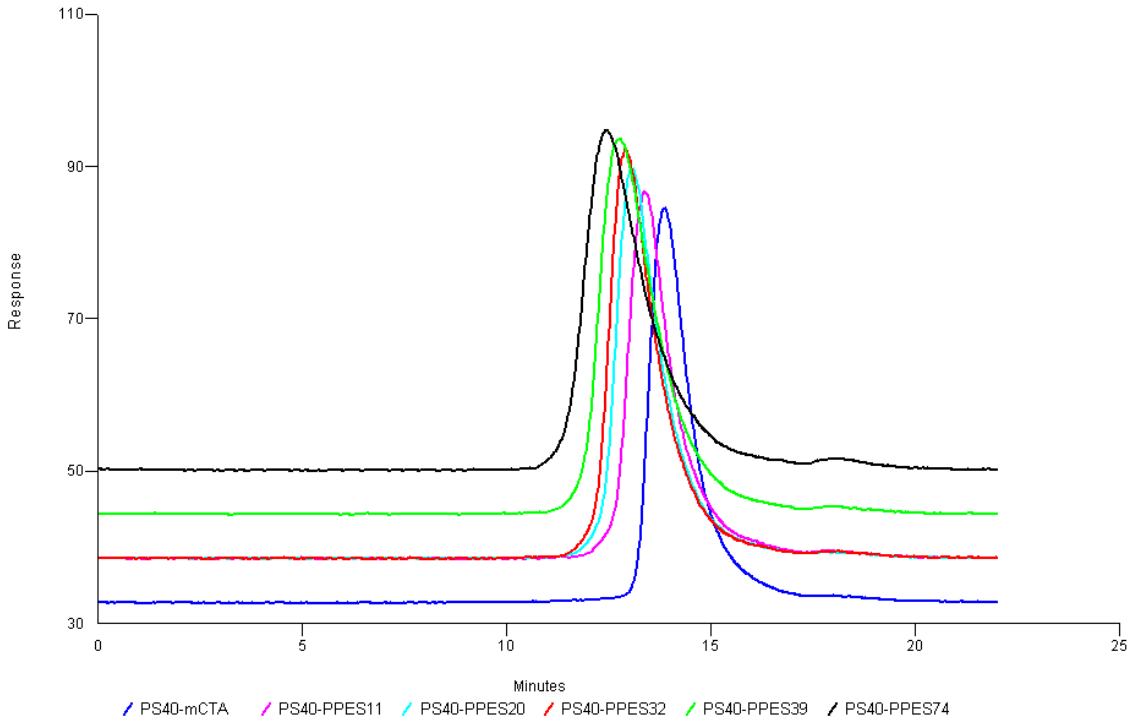

Figure A11. GPC profiles for PS-*b*-PPES copolymers, PS_{40} series with its parent mCTA.

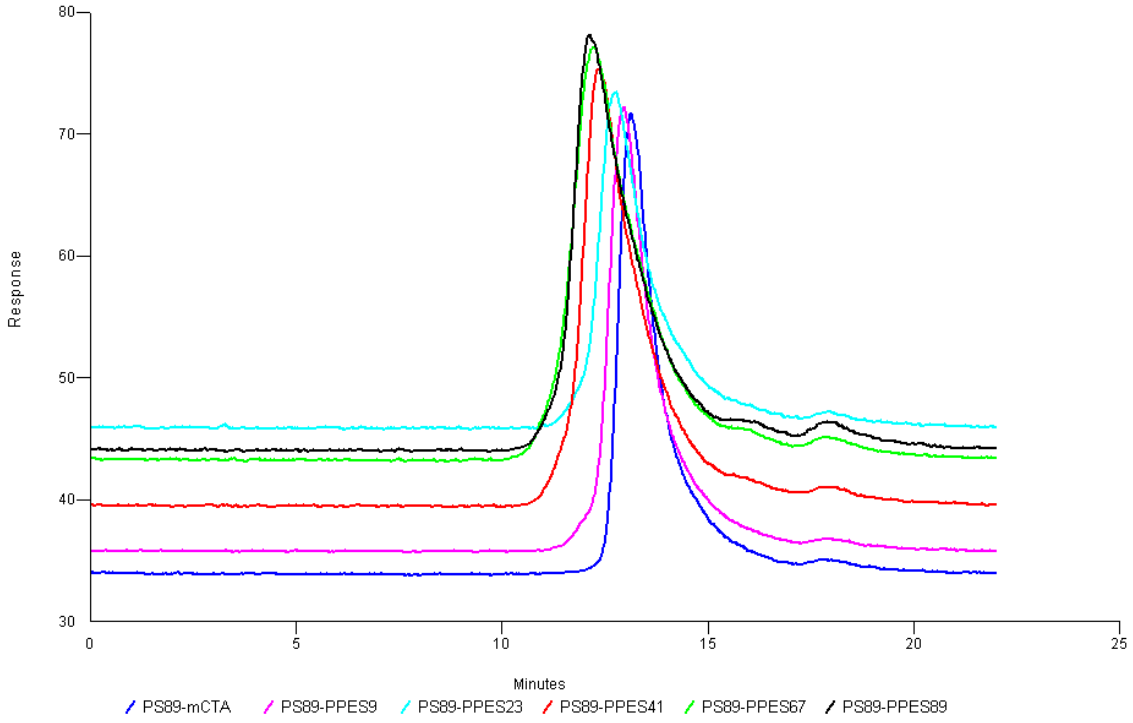

Figure A12. GPC profiles for PS-*b*-PPES copolymers, PS_{89} series with its parent mCTA.

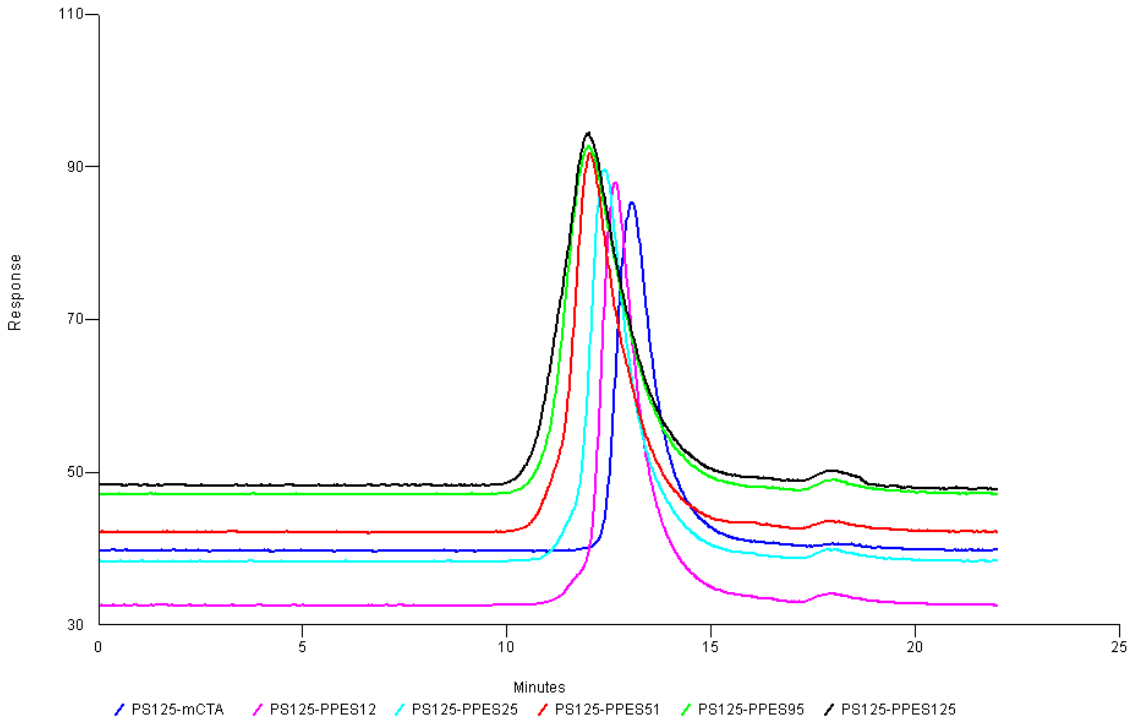

Figure A13. GPC profiles for PS-*b*-PPES copolymers, PS_{125} series with its parent mCTA.

Conversion Calculation by ^{1}H NMR

Figure A7 and A8 show the comparable ^{1}H NMR spectra for the synthesis of PS_{40}-mCTA. By setting the integral of the DMF methyl peaks (δ 2.96, s, CH_3; δ 2.88, s, CH_3) as constant, the change in area under styrene vinyl proton peaks (δ 5.82, d, *trans* CH_2=CH-; δ 5.31, d, *cis* CH_2=CH-) could be observed from initial crude (Figure A7, reaction time = 0 h) to final crude (Figure A8, reaction time = 141 h). Then we could calculate the conversion by equation (A1):

$$\boldsymbol{Conversion} = \frac{\boldsymbol{M_i - M_f}}{\boldsymbol{M_i}} \qquad \text{(A1)}$$

Where M_i is the initial integral of styrene signal and M_f is the final integral of styrene signal. The conversion of PS_{40}-mCTA polymerization is 60% (reaction time = 141 h) and the other mCTAs are calculated as same method.